ANL-7622

Argonne National Laboratory

AN INVESTIGATION OF FAST-REACTOR FUEL TESTING IN THE ENGINEERING TEST REACTOR (ETR)

by

J. C. Carter

Printed in the United States of America
Available from
Clearinghouse for Federal Scientific and Technical Information
National Bureau of Standards, U. S. Department of Commerce
Springfield, Virginia 22151
Price: Printed Copy $3.00; Microfiche $0.65

ANL-7622
Reactor Technology

ARGONNE NATIONAL LABORATORY
9700 South Cass Avenue
Argonne, Illinois 60439

AN INVESTIGATION OF FAST-REACTOR FUEL TESTING IN THE ENGINEERING TEST REACTOR (ETR)

by

J. C. Carter

Reactor Physics Division

November 1969

TABLE OF CONTENTS

TABLE OF CONTENTS

TABLE OF CONTENTS

LIST OF FIGURES

LIST OF TABLES

AN INVESTIGATION OF FAST-REACTOR FUEL TESTING IN THE ENGINEERING TEST REACTOR (ETR)

by

J. C. Carter

ABSTRACT

This is a report on preliminary work done in connection with the proposal to investigate possible mechanisms for failure propagation in assemblies of fast-reactor fuel elements. The fast-reactor environment is approximated by placing the assembly of fuel elements, surrounding by a neutron filter, in the experimental thermal reactor of the Idaho Nuclear Corporation.

The aspects of the work that are reported on are (1) the effect of the number of fuel elements in an assembly upon power densities, and (2) the effect of varying enrichment upon power distribution over any cross section of the assembly. The means of minimizing the power variation over the cross section of individual fuel elements and the characteristics and location of the neutron filter that surrounds the assembly are investigated.

The self-sufficient loop containing the assemblies will be placed in the J-13 space of the ETR. This loop contains a sodium pump and heat exchanger capable of removing 1.4 kW of heat from the 19 fuel elements.

Some safety aspects of the fuel-element assembly and filter are discussed, and the conditions at test shutdown are estimated.

This preliminary work indicates that there are no major technical problems in the design and testing of assemblies of fast-reactor fuel elements in the ETR and that the supporting facilities for the loop are adequate.

I. INTRODUCTION

This is a report of work done preliminary to the design and testing of assemblies of fast-reactor fuel elements for the Fuel Element Failure Propagation Program of the Metallurgy Division of Argonne National Laboratory.

The long-term objective of the program is to determine if any structural and material faults or abnormal operating conditions exist that can result in a loss of structural integrity progressively from fuel elements to subassemblies, to core, to reactor containment and if mechanisms and/or feedbacks exist or can be designed that may limit the progressive deterioration once it is started.

The immediate objective of the program is to determine if a fast-reactor environment can be simulated in a sufficiently large assembly of fast-reactor fuel elements, to the extent that useful information can be obtained on the phenomena of fuel-failure propagation from element to element to subassembly.

It is the intention to deliberately introduce structural and material imperfections into the fuel elements and to vary their heating and cooling rates, in a search for those imperfections and operating conditions that can initiate an undamped abnormal operating phenomenon. If an undamped abnormal phenomenon can exist, it is of interest to know how far it propagates throughout the test assembly and with what results.

The assembly of fast reactor fuel elements is contained in a sealed loop, which is within a source of fast neutrons. The test fuel elements are similar to those currently being prepared for large UO_2-fueled fast reactors. The maximum number of elements in an assembly is limited to 37 neutronic, thermodynamic, and structural conditions.

The length of the fast-reactor fuel elements and the space available for handling the test loops precludes the use of any existing fast-reactor facility unless the reactors and the test loop are modified extensively. Since no fast reactor is capable of accommodating the assembly of fuel elements in question, a filter and a thermal reactor are used. The alternative of surrounding the assembly of fast-reactor fuel elements by a thermal-neutron filter and/or a converter and placing this assembly in a thermal reactor becomes a question of which available thermal reactor meets the neutronic specifications requiring the least engineering revision.

The thermal reactor, first of all, must be capable of producing the required heating conditions in the fast-reactor fuel. In addition, the test loop, the handling facilities, the space available for the loop, the ability to provide instrumentation, and the hot-cell facilities for disassembling the loops are evaluated and compared in selecting the reactor. The selection of the reactor is based on what is considered to be the best combination of available facilities.

Since many kinds of reactors might conceivably be used for the tests in this program, the suitability of existing fast and thermal reactors in the USA was surveyed, and their characteristics are tabulated in Appendix A.

The materials-testing reactors appear to be the best suited for the experiments of this program. A few of those listed in Appendix B meet most of the criteria for reactor selection. These are listed in Table I. Others have sufficient power density in the core, but do not currently have the availability or handling facilities required for the program, and also will require extensive modifications to make them suitable.

TABLE I. Suitable Reactors for the Test Program

Reactor	Avg Power Density		Test Hole		Flux Available in Test Hole, nv
	Fuel, kW/kg ^{235}U	Core, kW/liter	Active Core Length, ft	Cross Section, in.	
ATR	8,500	670	4	5.25 diam	Thermal, $>10^{15}$; Fast, 1.5×10^{15}
ETR	7,600	494	3	6 x 6	Thermal, 4×10^{14}; Fast, 2.5×10^{14}
GETR	6,200[a]	625[a]	3	3 x 3	Thermal, 2×10^{14}; Fast, 5×10^{14}
HFIR	10,640	2,000			
MTR	9,000	400	2	3 x 3	Thermal, 5×10^{14}; Fast, 5×10^{14}
ORR	4,700	200	2	3 x 3	Thermal, 3×10^{14}

[a]Estimate for 50-MW operation.

The research reactors of the pool type generally have very low power. An analysis of the Babcock and Wilcox Test Reactor (BAWTR), which has one of the highest fluxes available in a pool reactor, is included to show some of the problems encountered with this kind of facility. Most of the power demonstration reactors listed in Appendix A are shut down or dismantled. An operating reactor should be used because of the high costs of new ones, reactivation, and semicontinuous operation. Transient reactors, such as the Transient Reactor Test Facility (TREAT), Power Burst Facility (PBF) represent another class in which some experiments may be conducted.

From the survey of existing reactors that may be available, the Engineering Test Reactor (ETR) is considered to be the most suitable for conducting fuel-failure propagation tests on assemblies of fast-reactor fuel elements from the standpoint of high flux, loop handling facilities, licensing, and sodium/water safety assessment.

Up to 37 pins in a suitable package loop can be physically accommodated in this reactor without modifying the core. Some difficulty with scheduling and availability may be encountered, but these problems are expected to be slight. Since the coolant diverger and many experiment hangers are located above the core, installing the test loop may be somewhat awkward. However, proper design should be able to circumvent this problem.

It is theoretically possible to install in the ETR a loop with a thermal-neutron filter and obtain the desired heat-generation rates without serious flux depressions. The total test-reactor power required is very high, resulting in high operating costs and low reactor utilization; i.e., a large portion of the test reactor may be tied up with the fast-reactor fuel test. The basic reason for this is that the filter removes the thermal neutrons whose production has been optimized in the reactor design, so that a satisfactory fast flux in the test region requires that the ETR run near full power during the test. For most of the contemplated experiments, a heat-generation rate of at least 2000 W/cc of UO_2 is desired. The type of other test loops or capsules in the core at the time the fast-reactor fuel test loop is to be placed in the reactor affect the nuclear conditions prevailing on the fuel-failure propagation loop. The testing program for the ETR should be known at least six months in advance so the loop can be adjusted.

Four parameters can be manipulated to control the heat-generation rate in the fuel elements. They are (1) the design of the filter and/or converter, (2) the loading of the ETR core, (3) the enrichment of the fuel to increase fission in the fuel and to control the flux depression, and (4) the power of the ETR.

Current order-of-magnitude estimates based on information furnished by the loop designers and the reactor operators indicate that the ETR can theoretically simulate the thermal conditions desired in the fast-reactor fuel elements of this test loop.

The position selected is the 6- x 6-in. J-13 hole, for which the following are estimated:

Thermal flux	3.5 to 4×10^{14}
Fast flux	2 to 2.5×10^{14}
Epithermal flux	4×10^{14}
Cadmium ratio	8

The required epithermal flux estimated for the fuel elements is on the order of 10^{14}.

II. DESIGN CRITERIA FOR FAST-REACTOR FUEL TESTING

A. Design Criteria for Test Loop

The function of the test loop is providing, in conjunction with an ETR, a nuclear and thermodynamic environment similar to that which exists within the core of a fast reactor.

The fuel elements and coolant in the test loop have no direct connection to the reactor system. The fuel elements have nuclear coupling by virtue of the fact that the filter and containing shell surrounding the assembly of fuel elements permit the passage of epithermal neutrons. The heat from the fuel elements is removed by a sodium-circulation system integral with the test loop and having no coupling to the reactor or any of its auxiliaries. Figure 1 is a schematic drawing of the loop and the reactor. The loop is in the form of a closed circuit around which sodium is circulated. The loop

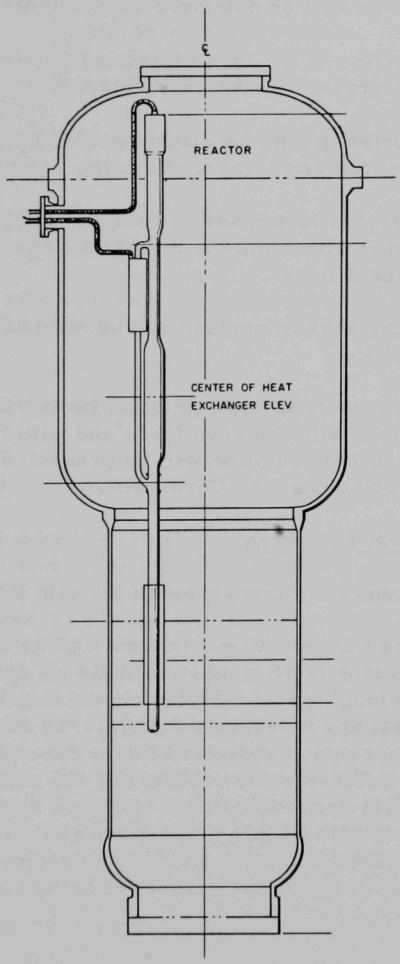

113-2820 Rev. 1

Fig. 1. Schematic Sketch of Test Loop in ETR

is positioned so the longitudinal midpoint of the fuel element in this loop is at the midpoint of the core section of the reactor. The length of the fuel element is equal to the length of the core.

The principal criteria are:

1. The walls of the loop must be capable of containing the maximum pressure that can occur within the loop. The maximum pressure that can conceivably occur will be determined by out-of-reactor experiments.

2. The section of the loop containing the assembly of fuel elements must be able to fit into the test hole of the reactor.

3. The sodium pump, heat exchangers, and auxiliaries must be an integral part of the loop and located above the reactor.

4. The integral loop must be designed so that it can be moved in and out of the reactor with a minimum of coupling and decoupling of coolant and instrument lines.

5. Since the sodium coolant will become activated, the loop must have adequate shielding.

6. The loop must be instrumented so that information obtained will be commensurate with the need for it and with the effort expended in obtaining it. This instrumentation will be presented in detail in subsequent design reports by Idaho Nuclear Corporation.

B. Criteria for Test Facilities

The most important component of the test facilities is the reactor.

The criteria for selecting a reactor and its auxiliary facilities are as follows: the reactor facility must (1) have an epithermal flux greater than 10^{14} nv at the longitudinal midpoint of the test location; (2) have a vertical in-core test space larger than $2\frac{1}{2}$ in. in diameter and 24 in. long; (3) have enough clear space above and below the core to install the test loop; (4) have the necessary availability for the scheduling of experiments; (5) have a reasonable operational cost; (6) have space and facilities for essential instrumentation; (7) have adequate radiation shielding; (8) have adequate safegrounds against a sodium water accident; and (9) have licensing and approval problems capable of being solved in a reasonable time.

Specifically, the reactor facility must meet the following requirements:

1. Producing heat generation in the fissionable material of the assembly of fuel elements at the rate of at least 2000 W/cc of fuel. The fuel may be any isotopic combination of plutonium and uranium oxide. The first fuel will be UO_2.

2. Pumping 500°C sodium in a longitudinal direction through an assembly of 19 fuel elements at the rate of 30 ft/sec.

3. Removing at least 1500 kW of heat from this sodium.

4. Providing a test hole longitudinally through the reactor of at least $2\frac{1}{2}$ in. in diameter.

5. Physically moving the integral test loop in and out of the reactor and to the hot cell with ease and safety.

6. Providing adequate space and facilities for instrumenting, measuring, and recording the performance of the test specimen while it is within the reactor.

The reactors that meet most of these requirements are discussed in Appendix B.

C. The Fuel Elements

Table V (later) lists the dimensions and volumes of the fuel elements that will be in the first test. The relative isotropic content can vary with each test up to 93% ^{235}U. For later tests in the program, some of the uranium may be replaced by plutonium. The actual amount of PuO_2 used will depend on the prevailing design of fuel elements for a Liquid Metal Fast Breeder Reactor (LMFBR) at that time. The high-density pelletized UO_2 is stacked to give an active length of 91.4 cm. This total length could be cut down to match the active length of any test reactor, but 91.4 cm is a more desirable length, since it matches the proposed core length of an LMFBR and of the ETR. The UO_2 will be canned in Type 304 stainless steel with 0.635-cm outer diameter and 0.039-cm wall thickness. The fuel-pellet diameter will be sized to give an 85% smear density. Each fuel element will have a gas plenum, and the overall length will be 137 cm.

III. DESCRIPTION OF THE TEST LOOP AND ITS TEST SECTION

A. The Test Loop

The design and fabrication of the test loop are the responsibility of the Idaho Nuclear Corporation. A detailed description (with drawings) is contained in report ANL/MET-03.[1]

B. The Test Section

The design of the test section of the loop is the joint responsibility of the Idaho Nuclear Corporation and the Metallurgy Division of Argonne. This design is in the preliminary stage.

The basic concept of the test section is that of an assembly of cylindrical fast-reactor fuel elements through which the sodium flows longitudinally. This assembly is surrounded by concentric regions of sodium, boron steel filter, and pressure shell. (Figure 2 is a schematic sketch of the test section.)

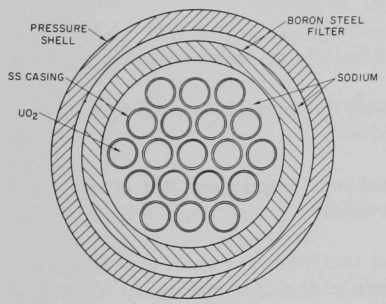

Fig. 2. Schematic Sketch of Test Section

The fuel elements are arranged on a triangular lattice with a 0.864-cm pitch. This pitch gives a 0.228-cm minimum flow annulus between the fuel elements. This annulus is a little larger than that of the Fast Flux Test Facility (FFTF) (0.16 cm) and on the small side of the 1000-MWe LMFBR designs (0.228-0.318 cm). With these specifications, the inner diameter of the test section is 1.110 in. A shroud around the seven pins directs the sodium flow and provides the coolant channel. This shroud is made up of two 0.076-cm-thick concentric tubes, separated by a 0.076-cm gas gap to act as a heat barrier in order not to cool the wall of the inner tube. Next is the inlet sodium annulus, which is bounded on the outside by the primary pressure vessel, rated at 1500 psi. This high-pressure rating is desirable in the light of recent TREAT experiments in the Mark-I loop.

The average power generation in this test section is 20 kW/ft of fuel element. For a 19-fuel-element, 91.4-cm-long bundle, the total power output is 1140 kW steady state. One series of tests to be made in this loop may involve increasing the power on a ramp to a maximum of 40 kW/ft of fuel element or 2280 kW total. The sodium velocity of 610 cm/sec requires about 52 psi head from the pump; allowing 42 psi for the in-core portion of the loop, and 10 psi for the remainder. A helical induction pump having a shutoff pressure of ~185 psi is used.

C. Loop Size for Other Numbers of Fuel Elements

For tests involving fewer than 19 fuel elements, the most economical solution would be to use the 19-fuel-element section with dummy fuel elements in the excess volume. This would result in using only one loop design and the same pump and would provide flow channels of the proper shape to maintain flow simulation.

Although most of the tests are to be made with 19 fuel elements, a larger number of fuel elements may be required in the later stages of the test program.

Some descriptive numbers pertaining to a preliminary concept of the test loop and test section are tabulated in Table II.

TABLE II. Descriptive Numbers for the Loop and Its Test Section

Dimensions of Loop	
Length	810 cm
Outside diameters	
In-core section	12 cm
Heat-exchanger section	24 cm
Pump and motor section	30 cm
Weight of loop	5000 kg
Test Section	
Number of fuel elements	19
Length of fuel elements	91.4 cm
Diameter of fuel elements	0.620 cm
Pitch of fuel elements	0.865 cm
Dimensions of Filter	
Length	91.4 cm
Inside diameter	6.0 cm
Outside diameter	7.3 cm
Loop Operating Conditions	
Heat removed through heat exchanger	1400 kW
Sodium flowrate	100 gpm
Maximum total pump pressure	700 g/cm^2
Sodium temperature	
Entering	500°C
Leaving	650°C
Materials of Construction	
Liquid-metal containment vessel	Type 316 stainless steel
Helium containment vessel	Type 316 stainless steel
Secondary-coolant containment vessel	Type 316 stainless steel
Water jacket	Aluminum
Thermal-neutron filter	Boron steel 2 wt %
Utility Requirements	
In-pile loop operations	
Electrical	480-V, 3-phase, 50-A, 60-cycle
Instrument air	100 psig
Helium	5800 cfm at 600 psig

TABLE II (Contd.)

Utility Requirements (Contd.)	
Hot-cell operation	
Electrical	480-V, 3-phase, 50-A, 60-cycle
Instrument air	100 psig
Clean process air	800 cfm @ 5 in. water
Process water	Negligible
Helium	2 cylinders per week
Hot liquid waste disposal	50 gal/month
Crane Requirements	
Above reactor vessel	
Capacity	40 and 2 tons
Headroom	30 ft
Hook travel	30 ft
Above canal	
Capacity	2 tons
Headroom	30 ft
Hook travel	50 ft
In hot-cell area	
Capacity	40 tons
Headroom	30 ft
Hook travel	30 ft

IV. DESCRIPTION OF ETR

The ETR is designed to perform engineering tests on fuel elements and components of nuclear plants. To make these tests under conditions simulating the actual proposed application, the following requirements must be met: (1) The reactor generates very high thermal and fast flux in the core test holes; (2) these holes in the core (high flux zone) range in size from 3 x 3 x 36 in. to 9 x 9 x 36 in.; (3) there is reasonable uniform flux from top to bottom of the core; and (4) the reactor is designed to contain closed-loop-type facilities for circulating any fluid coolant, including liquid metal.

The above requirements result in a reactor in which all experimental facilities are vertical and are inside the reactor vessel. The reactor control-rod drives are mounted below the reactor bottom head, where they are least affected by the experimental facilities. This arrangement is used because the upper vessel area is too congested with experimental-facility tubes, hangers, and other associated equipment to permit the use of control drives extending downward from the top head. Because of the large clear height needed to remove experimental apparatus, the vessel top was established near floor level. The depth of the vessel, the position of the core, and the biological shield, are determined by allowable radiation and biological considerations.

The ETR facility is a complete nuclear-engineering test facility. The design parameters and general data are given in Table III.[4] The reactor is light-water cooled and moderated and has a thermal rating of 175 MW. It is housed in a 112- by 136-ft gastight building, extending 58 ft above and 38 ft below grade. The reactor vessel consists of the multidiameter vessel proper, a removable elliptical dome (with flat top flange), a flat bottom head, a discharge chute, an inlet-water flow distributor, experimental hanger supports, experimental access nozzles, and the process-water inlet- and outlet-line connections. The vessel contains the reactor core and provides radiation space and facilities to accommodate the in-pile tubes to be used for nuclear-radiation experiments. Facilities also are provided for control rods, instrumentation, shielding of the vessel walls, directing coolant flow through the core, and support of all internal structure. Design pressures and temperatures of the stainless steel-clad carbon steel and stainless steel reactor vessel are 250 psig and 200°F. Operating pressures and temperatures are 200 psig and 110°F at the inlet and 150 psig and 133.5°F at the outlet.

TABLE III. ETR Design Parameters and General Data[4]

General	
Type	Thermal heterogeneous
Location	National Reactor Testing Station, Idaho
Purpose	Materials testing
Status	Went critical Sept 1957 and has operated at full power approx 50% of the time since
Total reactor power	175 MWt
Thermal-neutron flux	1.6-5 x 10^{14} n/cm^2-sec
Epithermal-neutron flux	5-15 x 10^{14} n/cm^2-sec
Fuel	Uranium-93% ^{235}U
Amount of ^{235}U in core	23 kg
Core height, active	91.44 cm
Average specific power	7600 kW/kg U
Power density	494 kW/liter of core
Metal-to-water ratio	0.67
Poison contents, natural boron	150 g

TABLE III (Contd.)

Core filler pieces (corner filler pieces)		4
Aluminum-reflector thickness		7.71 cm
Fuel Assemblies		
Number in core	Design Jan 1963	49 52
Length of assembly		137.32 cm
Size of assembly (approx)		7.62 x 7.62 cm
Fuel plates per assembly		19
Thickness of fuel plate		0.127 cm
Length of fuel plate		93.98 cm
Spacing between fuel plates		0.119 in. in 4 outer channels 0.115 in. in 2 channels 0.105 in. in 12 inner channels
Thickness of Al cladding		0.015 in.
Thickness of U-Al-B Alloy		0.020 in.
Core life before refueling	Design (present)	3500 MWd 5000 MWd
Vertical max/avg power ratio in fuel		1.4
Horizontal max/avg power ratio in fuel		1.7
Core max/avg power ratio in fuel		2.4
Initial excess reactivity		8 to 11%
Control-rod worth		
Black, total	Design (present)	14.4% 6%
Shim, each	Design (present)	1% 0.4 to 4%
Pressure at reactor tank inlet		200 psig

TABLE III (Contd.)

Core pressure drop	Design (present)	40 psig 43 psig
Coolant inlet temperature at reactor		110°F
Coolant outlet temperature	Design Jan 1963	138°F 133°F
Number of flow passes through reactor		1
Total coolant flow	Design (present)	44,400 gpm 51,000 gpm
Flow in fuel assemblies		29,700 gpm
Flow in control rods		6100 gpm
Flow in reactor		13,200 gpm
Heat-transfer area (core)		
Start of cycle		1350 ft^2
End of cycle		1439 ft^2
Average heat flux in fuel elements		0.453 x 10^6 Btu/hr-ft^2
Maximum heat flux (hot-spot factor 2.5)	Design (present)	1.15 x 10^6 Btu/hr-ft^2 1.7 x 10^6 Btu/hr-ft^2
Burnout heat flux		3.8 x 10^6 Btu/hr-ft^2
Maximum allowable fuel element surface temperature	Design (present)	280°F 400°F
Core and Reflectors		
Fuel-assembly array		10 x 10
Core lattice spacing: east-west, north-south		3.040 in.
Black rods in core		4
Gray rods in core	Design	10
Beryllium reflector geometry		
Inside dimensions		30.4 x 30.4 in.
Thickness		4.5 in.
Height		37.5 in.

TABLE III (Contd.)

Regulating rods in reflector	Design	2
Major experimental facilities in core		9
Major experimental facilities in reflector		8
Control Rods		
Type	Material	Number
Safety	Hafnium	4
Shim	Type A: Ni + 0.2% Co	12
Number of fuel plates per rod		16
Grams of ^{235}U per fuel follower assembly		184
Reactor Vessel		
Total height of vessel		35 ft 8 in.
Inside diameter of upper cylinder wall		11 ft 5 in.
Inside diameter of lower cylinder wall		7 ft 7 in.
Material		Stainless clad carbon steel and stainless steel
Thickness of upper cylinder wall		$2\frac{1}{4}$ in.
Thickness of lower cylinder wall		1 in.
Opening in ellipsoidal head		4 ft $6\frac{7}{8}$ in.
Opening in bottom head		5 ft 5 in. diameter
Thickness of bottom head		8.5 in.
Thickness of top flange		4.5 in.
Size of water-inlet pipe		36 in.
Elevation of water-inlet pipe		90 ft 9 in.

TABLE III (Contd.)

Size of water-outlet pipe	36 in.
Elevation of water-outlet pipe	83 ft 4 in.
Diameter of discharge chute	15 in.

The vessel internals consist of the inner tank, the internal thermal shields, the reactor core, the core support structure, and the experiment upper support ring. The core support structure consists of six structural supports extending from the reactor bottom head up to and including the support plate and the reactor grid plate. This structure supports the reactor core, the beryllium reflector, and the aluminum reflector, serves as a guide for the experimental in-pile tubes and control rods, and transmits the pressure-drop load across the core to the reactor bottom head.

The reactor core, a square configuration of 52 fuel elements, 12 shim control rods, four safety control rods, four corner filler pieces, and nine experimental facilities, is approximately 30.4 in. square.

The beryllium reflector is a $4\frac{1}{2}$-in.-thick layer of beryllium extending completely around the core. The two originally designed regulating rods were contained in holes on opposite sides in the beryllium reflector. Space also is provided in the beryllium for additional capsule-type experiments. The aluminum reflector pieces extend from the beryllium reflector out to the inner tank walls. Provision is made for eight experimental facilities in the aluminum reflector. Each aluminum reflector element is built with a hollow interior, providing for additional irradiation space of the capsule type.

The reactor vessel is enclosed and supported by a high-density concrete biological shield extending from the first floor to the basement ceiling. This shield is 8 ft thick at the core centerline. The 25-ft outside diameter of the shield is covered with a 3/4-in.-thick steel plate.

The subpile room is directly below the reactor bottom head. The walls of the subpile room (also of high-density concrete) transmit the biological shield load to the reactor foundations extending down to bedrock. The subpile room is the area in which experimental inpile tubes connect with the experimental piping, and this piping is routed to the experimental cubicles through access holes in the subpile room walls. The control rod, the regulating rod, and the chamber drives extend through the subpile room downward into the rod access room located directly below. The rod access room is located below the basement floor level, and is the area in which the control rod, regulating rod, and chamber drives are physically located and serviced.

The canal is T-shaped. The portion immediately west of the reactor is known as the working canal, and the north and south extensions are known as the storage canal. Fuel elements, control-rod sections, and certain experimental equipment can be discharged directly to the working canal through the reactor discharge chute. The working canal also provides storage for reactor handling tools and contains the canal saw used to remove end boxes from fuel elements or to saw other materials (including experimental equipment) to lengths suitable for further handling and shipment. The storage canal is used for storage of hot fuel, hot control fuel, miscellaneous experimental equipment, reactor equipment, baskets, slugs, canal bulkheads, and other items. Large casks for shipment of reactor fuel or experimental equipment also are placed in this canal for loading and/or unloading. The canal walls and bottom (constructed of ordinary concrete) are several feet thick to provide the necessary shielding for personnel working in the console and basement areas.

Material handling facilities include a 30-ton bridge crane, a 2-ton bridge crane, a $1\frac{1}{2}$-ton bridge crane, a freight elevator, a passenger elevator, two hatchways, and associated equipment. Individual experiments use various types of handling facilities, which, due to their specialized nature, are not discussed in this report.

V. NUCLEAR ANALYSIS

A. Introduction

At present, no facilities exist for testing assemblies of fast-reactor fuel rods in a fast-reactor environment. An alternative is the simulation of such an environment in a thermal reactor. This alternative method of testing requires a physical arrangement in which a small volume of fast-reactor fuel is placed in a large thermal core. Whether the fast-reactor fuel is surrounded by a neutron filter depends upon the extent of simulation required by the test.

If only the same average power density is desired over the cross section of each fuel element in an assembly, no filter is required. The desired power density can be obtained by varying the enrichment in each ring of elements inversely as the distance from the center of the assembly. However, the fission gradient on the diameter of each element is very steep.

If it is also desired to keep the fission gradient on the diameter of each element 20% or less, then a simple filter of uranium, boron, or cadmium is adequate.

If it is desired to simulate the fission spectrum of a particular fast reactor, it is theoretically possible to construct a filter by combining materials that have cross sections with the appropriate energy dependence to produce any desired spectrum. Such a filter is expensive and difficult to construct and requires experimental research.

This specific test program is based on assemblies of 7 and 19 fuel elements in the J-13 space of the ETR core.[2] It is desired that the fission rate over cross sections of the assembly and over the cross sections of individual fuel elements be less than 15 and 25%, respectively. Therefore, a neutron filter is required.

The intent is (1) to show how the principal parameters in the design of this type of test affect the phenomena occurring within the assembly, and (2) to present theoretical designs of a 7- and a 19-fuel-element assembly.

The principal parameters that can be varied are the number of fuel elements in an assembly, the enrichment of UO_2, the material of the filter, the thickness of the filter, and the diameter and pitch of the fuel elements in the assembly.

Preliminary calculations were made to show the effects of (1) the number of fuel elements in a test assembly, (2) the enrichment of the nuclear fuel, and (3) the material of the neutron filter. An estimate was made of the gamma heating in the fuel elements, in the neutron filter, and in the containment vessel. Preliminary designs of a 7- and 19-fuel-element assembly indicate that the desired power densities can be obtained in the test fuel elements when they are in the ETR.

The Advanced Reactivity Measurement Facility[3] (ARMF), may be used to measure nuclear parameters and to verify calculations. Measurements are being made in the Argonne Thermal Source Reactor (ATSR) to check filter materials and fission gradients in the proposed 7- and 19-fuel-element assemblies and in individual rods.

B. Basis of Calculations

The exploratory calculations were based on the following conditions:

1. The ETR is operating at 175 MW.

2. The J-13 core position is a square hole, 15.2 cm on a side and 91.4 cm long. Since this volume is larger than the volume of the test assembly, the excess area is assumed to be ETR core material. The assembly of fuel elements consists of a center fuel element surrounded by one or

more rings of fuel elements. For calculational purposes, the rings of fuel elements are converted to equivalent concentric cylinders. The equivalent surfaces and volumes are listed in Table IV. The four cylinders of UO_2 are equivalent to the center fuel element and to the rings of 6, 12, and 18 fuel elements. The UO_2 may be in combinations of regions 1, 3, 5, and 7. Filter material may be in region 5, 7, or 9, depending upon whether a 7-, 19-, or 37-fuel-element assembly is to be tested. Sodium and stainless steel may be distributed in regions 2, 4, 6, 8, and 9. (Region 10 is the ETR core.) The amount of stainless steel in a region is that contained in the cladding, spacers, and structural parts, with sodium occupying the remaining volume. The lateral surfaces and volumes of the UO_2 cylinders are approximately equivalent to the lateral surfaces and volumes of the fuel in the fuel elements they represent.

3. The values for ETR matrices and geometry are based on information given in Refs. 4.

4. The test assembly was assumed to be at the center of the ETR rather than in the J-13 core position. The effect of moving the test assembly from the center to the off-center J-13 position was determined by x-y calculations with the SNARG-2D code.

5. The codes used are SNARG-1D and SNARG-2D[5] with Cross-section Set 201[6] and DIF-2D[7] of the ARC system with Cross-section Set 203.[8] All codes give consistent results.

TABLE IV. Equivalent Cylindrical Volumes and Surfaces of Fuel-element Assemblies

	Regions of Test Assembly			
	1	3	5	7
Inside radii of regions, cm	0	0.849	1.750	2.223
Equivalent lateral surface of UO_2, cm^2	157.4	909.5	1861.8	2833.6
Equivalent volume of UO_2, cm^3	21.5	130.0	258.7	388.7

TABLE V. Dimensions and Volumes of UO_2 Fuel Element[a]

Length	91.44 cm
Cladding OD	0.635 cm
Cladding thickness	0.039 cm
UO_2 OD	0.548 cm
Lateral surface of UO_2	157.42 cm^2
Volume of fuel element and spacers	30.10 cm^3
Volume of cladding	6.67 cm^3
Volume of spacers	1.15 cm^3
Volume void	0.72 cm^3
Volume of UO_2	21.56 cm^3
Volume of ^{235}U and ^{238}U	10.57 cm^3
Vol % UO_2	71.63
Vol % stainless steel	25.98
Vol % void	2.39

[a]All dimensions at room temperature.

C. Number of Fuel Elements in an Assembly

The number of fuel elements that can be in an assembly and the length of these elements depend upon the reactor available, the characteristics of the fuel elements, and the power density required for the test.

The ETR has the highest flux and longest core of any reactor available. The fuel elements are similar to those anticipated for use in large thermal breeders. The maximum average power density specified for the test is 2000 W/cc of UO_2. The power density at the midpoint is 2600 W/cc of UO_2.

The J-13 space in the ETR core limits the test assembly to 37 UO_2 fuel elements. Each UO_2 pellet is 0.548 cm in diameter, and the total length of the pellets is 91.4 cm. The enrichment of the center fuel element is 93%. The enrichment of the ring of six is 85%, of the ring of 12 is 74%, and of the ring of 18 is 58%.

The effect of increasing the number of rings of fuel elements in a test assembly is that of successively increasing the shielding of the inner rings of fuel elements. This decreases both the magnitude of the fission rate in the fuel elements of each successive ring and the gradient of the fission rate along the diameter of a fuel element that is coincident with the radius of the assembly. No attempt has been made to calculate the angular distribution of fission rate in a fuel element except for the center fuel element. Experiments are under way to measure the angular and radial variation over cross sections of fuel elements in the rings of 6 and 12 fuel elements.

Table VI shows the effect of adding successive rings of 12 and 18 fuel elements to an assembly of seven fuel elements. All fuel elements are of the same enrichment. The filter material and thickness are maintained constant, but the filter diameter increases as rings of fuel elements are added. Power density was computed for the midpoint of 91.44-cm-long fuel elements with the assemblies so positioned in a reactor that the centerline, or the center fuel element, is coincident with the longitudinal centerline of the ETR core. The thickness of the cadmium filter is 35 mils. The filter is in region 5 for the seven-fuel-element assembly, in region 7 for the 19-fuel-element assembly, and in region 9 for the 37-fuel-element assembly.

TABLE VI. Power Density in Assemblies Containing 7, 19, and 37 UO_2 Fuel Elements

Center Fuel Element		Ring of 6 Fuel Elements		Ring of 12 Fuel Elements		Ring of 18 Fuel Elements	
Enrichment	W/cc UO_2	Enrichment	W/cc UO_2	Enrichment	W/cc UO_2	Enrichment	W/cc UO_2
93	4117	93	4886				
93	3175	93	3520	93	4495		
93	2641	93	2817	93	3256	93	4172
70	3099	70	3678				
70	2390	70	2649	70	3383		
70	1988	70	2120	70	2451	70	3140
50	2213	50	2626				
50	1707	50	1892	50	2417		
50	1420	50	1515	50	1751	50	2243
30	1328	30	1576				
30	1024	30	1135	30	1450		
30	852	30	909	30	1050	30	1346

As rings of fuel elements are added, the difference in power density between rings becomes less and the gradient on the radius of the assembly becomes less, indicating that low-energy neutrons are being captured in the outer rings of fuel elements. Since the outer fuel elements capture the largest percentage of low-energy neutrons, these fuel elements have the steepest fission gradient on the diameter that is coincident with the radius of the assembly.

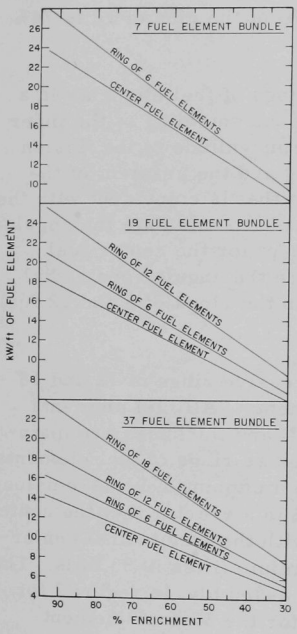

113-2684

Fig. 3. Heat Generation vs Percent Enrichment

D. Enrichment

The ability to vary the enrichment of the test fuel elements provides the primary means of obtaining the desired average fission rate per element throughout the assembly. A fairly uniform average fission rate for all fuel elements in an assembly is readily obtained by varying the enrichment over the assembly cross section. A uniform average fission rate over the cross section of individual fuel elements can be approached by using the minimum amount of enrichment per fuel element consistent with the requirements of the test, and by using a neutron filter that removes a large percentage of the epithermal neutrons as well as the thermal neutrons.

Figure 3 shows the heat generation of each fuel element in assemblies of 7, 19, and 37 fuel elements in the J-13 space plotted against the percent enrichment of the UO_2. Since the fission rate in an individual fuel

element is also affected by the position of the fuel element in the assembly and the nuclear properties of the neutron filter surrounding the assembly, many combinations of parameters are possible.

The power density in a fuel element and the power gradient on the diameter of individual fuel elements is presented for five cases. The cases are chosen to show the effect of (1) enrichment, (2) the number of fuel elements in an assembly, and (3) the neutron filter. The minimum fission rate in a center fuel element is at the center of that element. The minimum in all other fuel elements is at the point on the element nearest the center of the assembly. The effect of enrichment is illustrated by the following five cases and summarized in Table VII.

TABLE VII. Power Gradients in Fuel Elements

Case No.:	I		II		III		IV			V		
No. of fuel elements:	7		7		7		19			19		
Filter material:	Cadmium		Cadmium		Boron		None			Cadmium		
Filter thickness, mils:	35		35		96		-			35		
Fuel element in:	Center	Ring of 6	Center	Ring of 6	Center	Ring of 6	Center	Ring of 6	Ring of 12	Center	Ring of 6	Ring of 12
Enrichment:	50	44	30	26	93	93	93	93	93	93	93	93
W/cc of UO_2:	2420	2472	1547	1537	2290	2370	4421	5147	11360	3159	3511	4336
Radii, cm	Power-density Ratio											
0.2740	1.081	1.000	1.070	1.000	1.043	1.000	1.085	1.000	1.000	1.065	1.000	1.000
0.2055	1.039	1.001	1.034	1.002	1.021	1.001	1.040	1.002	1.020	1.032	1.001	1.010
0.1370	1.017	1.006	1.015	1.005	1.009	1.002	1.018	1.010	1.093	1.014	1.002	1.022
0.0685	1.004	1.023	1.003	1.020	1.002	1.005	1.005	1.025	1.150	1.004	1.012	1.043
0	1.000	1.036	1.000	1.031	1.000	1.012	1.000	1.049	1.297	1.000	1.023	1.067
0.0685	1.004	1.060	1.003	1.050	1.002	1.024	1.005	1.072	1.500	1.004	1.040	1.102
0.1370	1.017	1.091	1.015	1.080	1.009	1.037	1.018	1.121	1.666	1.014	1.065	1.138
0.2055	1.039	1.138	1.034	1.112	1.021	1.055	1.040	1.165	2.350	1.032	1.098	1.187
0.2740	1.081	1.179	1.070	1.159	1.043	1.078	1.085	1.262	3.465	1.065	1.131	1.237

Case I is a seven-fuel-element assembly with the enrichment varied to give approximately the same average power density in each fuel element. A 35-mil cadmium filter surrounds the assembly.

Case II shows how the level of power density in a seven-fuel-element assembly with the same filter as Case I affects the gradient of the power across the diameter of each fuel element.

Case III shows that an acceptable power gradient can be achieved with a high enrichment and a thick filter of boron. However, it is an expensive way to achieve the objective of low power gradient.

Case IV is a 19-fuel-element assembly with no filter. The point generated in each fuel element is that concomitant with operating the ETR at 175 MW. Such a condition would melt the fuel elements. It is possible to show what could happen if the filter was tested during a test of highly enriched fuel elements.

Case IV also shows the shielding effect of the outer ring on the fission gradient in the inner fuel elements in the absence of a neutron filter. A comparison of Cases IV and V shows how a filter alters the

fission distribution in rings of fuel elements. The filter is necessary in order to attain a low gradient of power density over the cross section of a fuel element, especially if the fuel element is highly enriched. The low power gradient is achieved by increasing the percentage of fissions in the high-energy groups.

Varying the enrichment, filter thickness, and ETR power can produce the desired power level and power gradient.

E. Neutron Filter

Filter materials with a high-neutron-absorption cross section for low-energy neutrons are desired. Theoretically, rare earths such as europium, samarium, dysprosium, and erbium appear attractive as filter materials.[9] They have large resonance integrals, with the resonances closely spaced so that large average cross sections well into the keV range are produced. There is essentially no burnup problem with these materials, since neutron absorption produces another rare-earth isotope, usually with a large cross section.

Materials such as tantalum and rhenium are also potential filter materials because of high melting points and good absorption cross sections at low energies. Their cross sections are not as high as those of cadmium, boron, and the rare earths; therefore, filters of these materials must be thicker than filters of cadmium, boron, and the rare earths, thus creating heat-transfer and space problems.

Materials such as cadmium with low melting points are a potential source of trouble, because the sodium temperature in the test assembly is not less than 500°C. The actual choice of a filter is a compromise of performance, economics, and safety. At present, cadmium oxide and boron steel appear to be the best filter materials.

A uranium filter, when removing its fission heat is feasible, has the unique advantage of being able to provide a heat-generating boundary for the flowing sodium, thus enhancing the chances of attaining dynamic similarity between a small test assembly and a large fast reactor.

Cadmium absorbs almost all the neutrons below 0.41 eV and allows nearly all the higher-energy neutrons to pass through. Cadmium offers little flexibility in altering the epithermal flux. Figure 4 shows the effect of the thickness of cadmium on the power density in 93%-enriched UO_2 fuel elements in a seven-fuel-element assembly. The optimum thickness of pure cadmium appears to be 35 mils. Any thickness above 35 mils appears to have little effect on the power density.

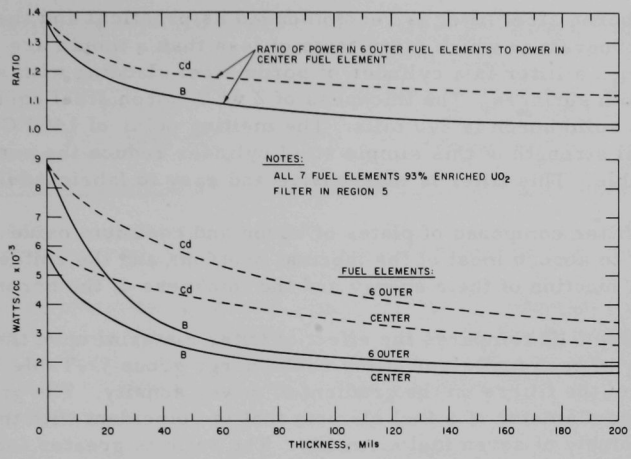

113-2685

Fig. 4. Effect of Filter Thickness upon Power in a Seven-fuel-element Assembly

The gamma heating of cadmium is estimated to be 15 W/g of cadmium. The gamma heating would be approximately 80 kW for a 35-mil cadmium filter. The cadmium filter must be formed of cadmium oxide, because pure cadmium melts at 321°C. The cadmium oxide filter absorbs almost all the thermal neutrons, but has no flexibility in controlling the high-energy neutrons. Its melting point is 1426°C. The thickness equivalent to 35 mils of pure cadmium is 50 mils. The filter would probably be a thin cylinder of cadmium oxide clad with stainless steel.

Boron is a 1/v absorber that is stable at high temperatures. Therefore, boron offers more flexibility than cadmium in controlling the neutron spectrum. Figure 4 shows the effect of the thickness of the boron on power density in a 93%-enriched UO_2, seven-fuel-element assembly.

The irradiation of boron produces helium. The ^{10}B (n,α) reaction is undesirable, but must be considered along with the effect of irradiation upon the structural integrity. For the anticipated test time in the ETR, the irradiation effects do not seem to present insurmountable problems. The heat to be removed from the boron is estimated at 20 W/g. This is slightly higher than for cadmium because of the energy of the (n,α) reaction in addition to the gamma heating.[10]

A boron filter may be boron between plates of stainless steel or simply an alloy such as boron steel, zirconium-boron, or titanium-boron. If the filter consisted of both boron and cadmium, nearly all neutrons of thermal energy would be filtered out by the cadmium, and as many of the epithermal neutrons as desired could be filtered out by varying the amount of boron.

A boron steel filter is recommended as practical and the safest for a testing program in which many tests of less than a month are to be conducted. Such a filter is a cylinder of boron steel cladding with stainless steel on both surfaces. The thickness of 2 wt % boron steel equivalent to 15 mils of solid boron is 240 mils. The melting point of 1400°C and the mechanical strength of this simple steel cylinder reduce the possibility of filter trouble. This filter is inexpensive and easy to fabricate in quantity.

A filter composed of plates of boron and cadmium oxide combines the ability to absorb most of the thermal neutrons and the epithermal neutrons as a function of their energy and the thickness of the boron plate.

Table VIII compares the effect of filter material upon the average $\phi\Sigma_{fj}/\sum\phi\Sigma_f$ in each fuel element for each energy group j. Table IX shows the effect of the filters on the gradient of power density. The gradient is taken on the diameter of a fuel element that is coincident with the radius of the assembly of seven fuel elements. The ratio is greater for boron than for cadmium because, as stated, the thickness of filters is chosen so that the total power in the seven fuel elements is the same for all filters. Under this condition, the thickness of boron was such that more fissions occurred in the lower-energy groups when the boron filter was used than when the cadmium was used. (See Table VIII.)

TABLE VIII. Effect of Cadmium, Boron, and Uranium Filters upon $\phi\Sigma_{fj}/\sum\phi\Sigma_f$

Group	Energy Range	Lethargy, Range u	Δu	Center Fuel Element			A Fuel Element in the Ring of 6		
				Cd	B	U	Cd	B	U
1	10-3 MeV	0-1.204	1.204	2.88	3.12	4.11	2.28	2.38	3.48
2	3-1.4 MeV	1.204-1.966	0.762	6.07	6.45	8.22	5.02	5.22	7.03
3	1.4-0.9 MeV	1.966-2.408	0.442	2.26	2.42	3.51	1.93	2.13	3.00
4	0.9-0.4 MeV	2.408-3.219	0.811	2.47	3.83	5.02	2.94	2.97	4.20
5	0.4-0.1 MeV	3.219-4.605	1.386	4.32	4.33	5.92	3.65	3.90	4.49
6	100-17 keV	4.605-6.377	1.772	4.94	5.04	6.02	3.75	4.20	5.02
7	17-3 keV	6.377-8.112	1.735	6.07	6.14	6.62	5.37	5.52	5.92
8	3-0.55 keV	8.112-9.808	1.696	9.78	9.97	10.03	8.62	8.30	8.49
9	550-100 eV	9.808-11.513	1.705	16.93	16.61	13.04	16.12	14.54	11.53
10	100-30 eV	11.513-12.717	1.204	12.77	11.08	4.11	13.59	12.46	4.10
11	30-10 eV	12.717-13.816	1.099	10.92	9.16	3.01	13.89	12.00	3.50
12	10-3 eV	13.816-15.020	1.204	5.15	4.13	0.80	8.31	6.48	0.89
13	3-1 eV	15.020-16.119	1.099	12.25	7.15	10.53	11.46	6.52	9.92
14	1-0.4 eV	16.119-17.035	0.916	2.93	6.55	11.53	2.63	6.23	11.90
15	0.4-0.1 eV	17.035-18.421	1.386	0.26	3.52	7.02	0.30	4.47	11.02
16	Thermal	18.421		0.00	0.50	0.50	0.00	2.50	5.00

NOTES:
1. The power for the seven fuel elements with the cadmium filter is 302 kW.
2. The power of ETR is 175 MW.
3. The enrichment of the center fuel element is 54% and that of the element in the ring of 6 is 46%.
4. The fuel element is the one in Table V.

TABLE IX. Effect of Filter upon Maximum-to-Average Fission Rate in a Fuel Element

Center Fuel Element			A Fuel Element in the Ring of 6		
Cd	B	U	Cd	B	U
1.048	1.055	1.056	1.11	1.12	1.14

This investigation indicates that a variety of materials can be used as filters by varying their thickness, if a uniform heat-generating rate is the only requirement. If a particular spectrum is desired, the filter must be a composition of materials having cross sections of the appropriate energy dependence.

The choice of a filter is a compromise between performance and economics.

F. Gamma Heating

The gamma heating rate in a 19-fuel-element test assembly irradiated in the center of the ETR core has been estimated.[11] The gamma fluxes at the midplane of the five-region assembly were calculated using formulas for cylindrical geometry and a uniformly distributed source.[12]

Flux values were found for points at the center, halfway through the five-region assembly, outside the five-region assembly, and at the outer edge of the test assembly. Gamma radiation from the core region outside the test assembly was determined. This radiation was attenuated by the intervening material of the assembly before being absorbed at the designated points and contributing to the heating rates.

During irradiation, heating of the steel pressure vessel is calculated to be 15 W/g; heating of the cadmium filter surrounding the test assembly, 15 W/g. The calculated gamma heating in fuel elements in a test assembly is: central fuel elements, 25 W/g of UO_2; and ring of 12 fuel elements, 23 W/g of UO_2.

During irradiation, a major portion of the heating is produced by radiation from the surrounding core. Calculations show that immediately after the test assembly is removed from the ETR core, the equilibrium fission products in the test assembly produce 6 W/g of gamma heat in the five central regions of UO_2 and 2 W/g of gamma in the steel pressure vessel.

G. Preliminary Design of 7- and 19-fuel-element Test Assemblies

Calculations were made for assemblies consisting of 7, 19, and 37 fuel elements. However, only the 7- and 19-fuel-element assemblies were being considered for testing at this time.

The total power required per fuel element is assumed to be 45 kW. The average power density at the midpoint of each fuel element is then 2600 W/cc of UO_2. The neutron filter is equivalent to 35 mils of cadmium. The ETR is assumed to be operating at 175 MW.

1. A Seven-fuel-element Test Assembly

For the average power density at the midpoint of each fuel element to be 2600 W/cc, the calculated enrichment of the center fuel element must be 54% and that of the surrounding ring of six fuel elements must be 46%.

Figure 5 shows the 16 group fluxes throughout the assembly of seven fuel elements. Figure 6 shows the percent of fissions in each of 16 energy groups on the center fuel element and for fuel elements in the ring of six. Figure 7 shows the fission distribution among energy groups. Figure 8 shows the power variation on the diameter of the fuel element that is concurrent with the radius of the assembly.

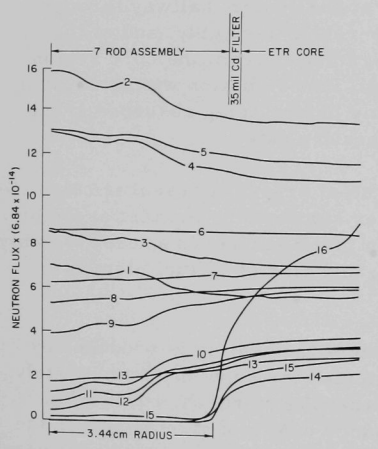

113-2695

Fig. 5. Flux Distribution as a Function of Radius in a Seven-fuel-element Assembly

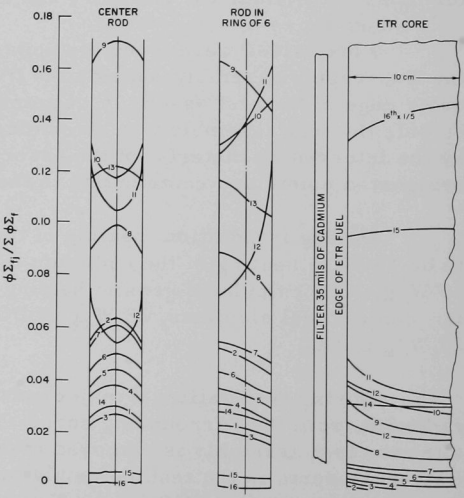

113-2699

Fig. 6. Fission Spectrum in Each Element of a Seven-fuel-element Assembly

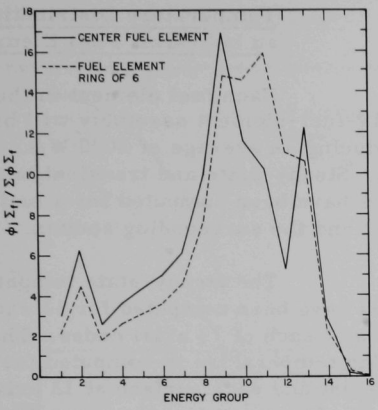

Fig. 7

Fission Distribution among Energy Groups for a Seven-fuel-element Assembly

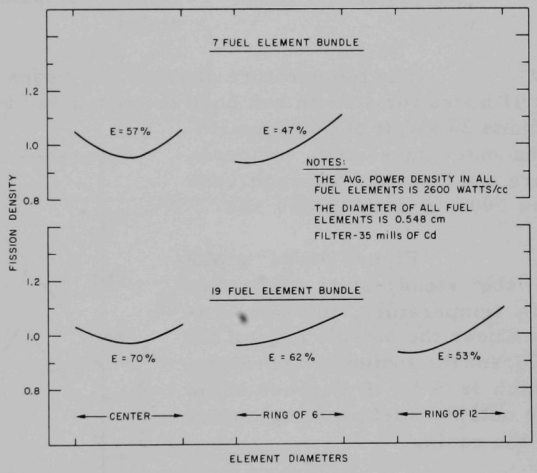

Fig. 8

Power Gradient on Diameters of Fuel Elements

2. A 19-fuel-element Test Assembly

For the average power density at the midpoint of each fuel element to be 2600 W/cc, the calculated enrichment of the center fuel element is 72%, the enrichment of the fuel elements in the ring of six is 65%, and the enrichment of the fuel elements in the ring of 12 is 55%. Figure 8 shows the gradients of power density for fuel elements in each ring. Figure 9 shows the percentages of the fissions averaged over the cross section of the fuel elements attributable to each of the 16 groups into which the energy spectrum is divided.

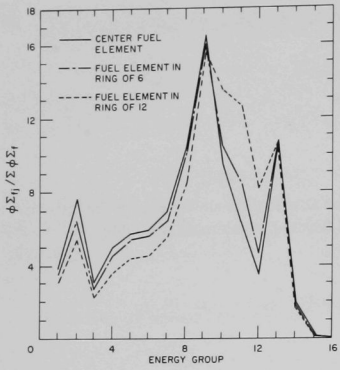

113-2696

Fig. 9. Fission Distribution among Energy Groups for a 19-fuel-element Assembly

3. Temperature Distribution in an Individual Fuel Element

Each fuel element in the 7- or 19-fuel-element assembly will be producing an average of 2000 W/cc of UO_2. Steady-state and transient temperatures have been computed for a fuel element and the surrounding sodium.

The steady-state temperatures have been computed for 11 radial nodes at each of 13 axial nodes. The casing temperature is computed for the midpoint and each surface at 13 axial nodes. The average sodium temperature is computed for each of 91 axial nodes.

The temperature at these 143 nodes for the UO_2 and casing and at 91 nodes for sodium has been computed and is available for powers of 15 and 20 kW/ft of fuel element. The entering-sodium temperature and flowrate for each case are 500°C and 450 g/cm^2 sec.

Figure 10 is a plot of the steady-state centerline UO_2 temperature, the temperature near the outside edge of the UO_2, and the sodium temperature, which is 5 to 10 degrees below the outside surface temperature of the casing.

Figure 11 is a plot of the steady-state radial temperature at the midsection of the fuel element.

The transient temperature at the above nodes have been computed for 15 and 20 kW/ft of fuel element. In addition, the percentage of UO_2 melted and the time at which sodium starts boiling have been computed. Figure 12 shows the results for a power ramp of 3.21 in 0.2 sec. The entering-sodium temperature and flowrate are 500°C and 450 g/cm^2 sec.

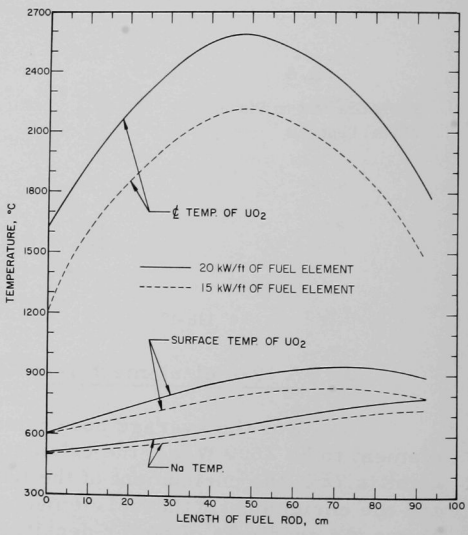

113-2682 Rev. 1

Fig. 10. Steady-state Axial Temperature in a Fuel Element

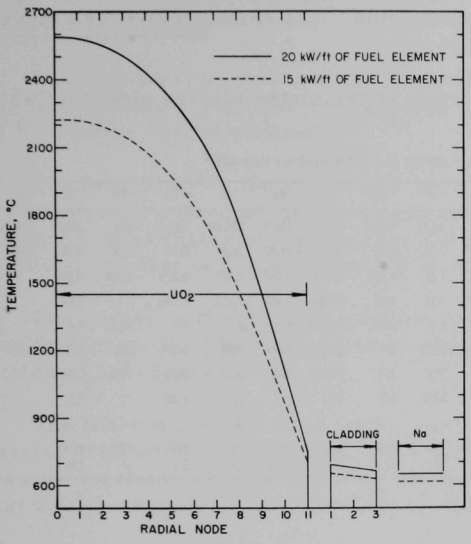

113-2683 Rev. 1

Fig. 11
Steady-state Radial Temperature in a Fuel Element

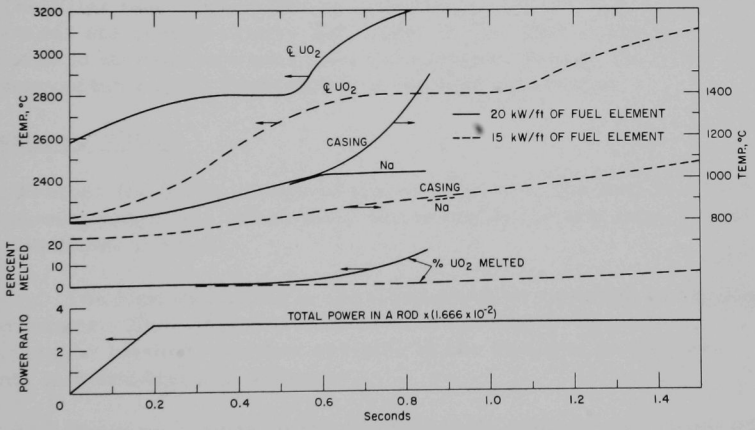

113-2691 Rev. 1

Fig. 12. Transient Temperature Distribution on the Centerline of a Fuel Element

Figures 10-12 show what type of information can be calculated as the design of the test loop evolves. Producing the data on each figure takes about 10 to 15 min computing time. The calculations were made using the heat-transfer module of SAS1A.[13]

The physical properties of the materials are given in Table X.

TABLE X. Physical Properties of Possible Assembly Materials[14]

Material:	UO_2	SS	Na	B	Cd	Hf	Re	Ta	Dy	Eu	Gd	CdO	BN
Molecular weight	268		23	10.82	112.41	178.6	186.3	180.88	162.46	152	156	128.41	24.83
Density, g/cm^3	10.00	7.92	0.97	2.34	8.65	13.29	21.02	16.6	8.54	5.26	7.90	6.95	2.30
Specific heat, W-sec/g°C	0.395	0.581	0.700	1.28	0.230	0.147	0.137	0.195	0.173	0.166	0.299		0.540
Thermal conductivity, W/cm°C	0.039	0.225	1.328	0.92	0.48	0.205	0.545	0.754	0.094		0.088		0.20
Coeff. of linear expansion x 10^6	13.46	21.6	71	8.3	29.8	5.90	6.6	0.8	8.6	32.0	6.4		8.0
Melting temp, °C	2800	1500	98	2300	321	2130	3180	2996	1407	826	1312	1426	2730
Vaporizing temp, °C	3200		883	2550	767	5400	5900	6100	2600	1439	3000		
Young's modulus, psi x 10^{-6}	20.0	29.0		64.0	8.0	20	67	27	9.15		8.5		8.0
Poisson ratio	0.30	0.25						0.35					
Cross section, σ_a {barns	15.14	2.24	0.505	750	2450	105	86	21	950	4300	4600		
cm^2/g				42	12.9	0.39	0.23	0.07	3.5	17	176		

VI. NEUTRON FILTER

A. General Discussion

The low-energy neutron filter is designed to create neutronic conditions in the assembly of fast-reactor fuel elements as nearly like that of a fast reactor as can be attained.

The best filter is the result of a judicious balance between the ability to produce a desired fission spectrum, the rate of burnup of the atoms of the filter material, the mechanical properties of the alloy, the availability, the cost of filter materials, and the cost of fabrication.

The ability of the filter to produce the desired fission spectrum is treated in Section V. The burnup and mechanical properties are treated in Sections VI.C-E below.

The filter materials used in this test are readily available and inexpensive. The cost of fabrication is not known at this time, but should not be an important factor if cadmium or boron is used. If the rare earths are used, both availability and fabrication will be important factors.

The design and fabrication requirements for the filter are stringent. The filter must be uniform in dimensions, and the material must be homogeneous and free of cracks and voids. If the filter contains a region transparent to thermal neutrons, they will stream through the filter and cause unacceptable local overheating of the test specimens.

B. Location of Filter

Whether the filter is located inside or outside the loop is a matter of engineering judgment. When the filter is inside the test loop, the following conditions prevail:

1. The heat generated in the filter must be removed by the loop heat exchanger. This requires that the heat exchanger be larger; thus the heat exchanger becomes another variable in the decision on the power gradients in individual fuel elements.

2. The temperature of the filter is high, reducing the filter lifetime.

3. The filter must be of a material with a melting point higher than 700°C.

4. The diameter of the pressure shell is larger.

5. It is difficult to change the filter once it is installed.

6. It is impossible to use cadmium in the filter, because the melting point of cadmium is 301°C and the sodium temperature is not less than 500°C.

7. There is no moderator between filter and test section when the filter is located inside the loop.

When the filter is outside the test loop, the following conditions prevail:

1. The filter is easily changed without disturbing the test loop. This is an important consideration.

2. The filter is cooled by the reactor coolant, and no limitations are placed on the thickness of the filter or on melting points greater than 200°C.

3. Cadmium may be used exclusively or in conjunction with other materials to provide more flexibility in controlling the neutron energy spectrum.

4. There may be moderator between filter and test section, unless all the heat is removed from the outside surface of the filter.

At this time, the location of the filter has not been decided upon.

If the filter is located in the sodium it may be composed of an alloy of boron and austenitic stainless steel which has a ^{10}B concentration of 0.0084×10^{24} atoms/cc of a 2 wt % alloy. The filter alloy will be clad with stainless steel, or plated with some other suitable material to prevent excessive corrosion after an appreciable amount of burnup. If plating is used, careful selection and control of the method of plating will be required to ensure a good bond between the filter alloy and the plated material. The fittings at the ends of the filter are austenitic stainless steel.

If the filter is outside the loop, the material will most likely be 1 wt % boron steel. The reason for 2 wt % for the inner filter rather than 1 wt % is to reduce the thickness and the temperature gradients.

Boron was selected for the following reasons:

1. The absorption cross section of boron is inversely proportional to neutron energy, thereby fulfilling the functional requirement.

2. The cross-section curve does not have any resonances, precluding a possible source of difficulty and uncertainty in calculation.

3. Boron alloys have been fabricated and applied in a range of sizes, shapes, compositions, and isotopic enrichments, thus minimizing development and procurement problems.

The selection of the means of using boron as a filter material was, in part, a process of elimination. All ceramics were rejected on the basis of possible void formation during operation: fused ceramics, because of cracking; and powdered ceramics, because of thermal- or vibration-initiated redistribution. From the several cermet and alloy materials considered, borated stainless steel was selected. Boron carbide-stainless steel cermets appear at least as good as borated stainless steel, but less information on boron steel is available.

C. Atom Burnup[15]

The estimate of atom burnup is based on the filter being outside the test loop in a relatively cool environment. All irradiation burnup data were converted to boron atoms burned per cubic centimeter of alloy. The conversion of boron atoms burned (helium atoms formed) per cubic centimeter of alloy is similar to the approach taken in APDA-133.[16] Allowable burnup is assumed to depend on the gas pressure developed per unit volume of alloy. Figure 13 shows the allowable burnup at different temperatures for the 1% boron stainless steel filter in APDA-144.[15]

The right-hand scale of Fig. 13 is obtained by dividing the left-hand scale by the reference design ^{10}B concentration (52×10^{20} atoms/cc of alloy). For the maximum filter temperature of 154°C, the maximum allowable burnup is 20%. (See Section VI.E for determination of filter temperature.) Since the left-hand scale is divided by the ^{10}B concentration to obtain the right-hand scale, reducing the ^{10}B concentration in the alloy will increase the allowable burnup percent for the same allowable burnup in atoms/cc. Thus, reducing the boron concentration by one-half doubles the allowable percentage of burnup.

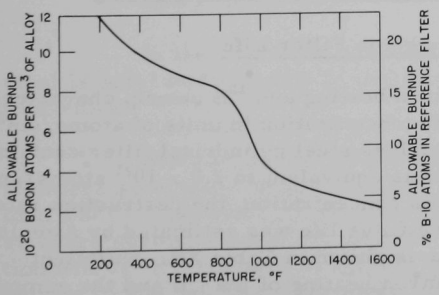

Fig. 13. Burnup Limitation of 1 wt % Boron-Stainless Steel Alloy

The allowable burnup for temperatures less than 230°C was derived from irradiation data in Ref. 17.

Since irradiation data are not available for boron stainless steel alloys at temperatures greater than 230°C, the data had to be obtained

indirectly. The boron in B-SS alloys has negligible solid solubility in iron. Boron compounds are formed with other elements in stainless steel, and the result is that the alloy is essentially a cermet, although the particle size and distribution is not ideal. Assuming that this alloy does not act as a cermet, convert the high-temperature data (above 427°C) for uranium oxide-stainless steel dispersions presented in APDA-133[16] to B-SS alloys. Since four times as many gas atoms are formed for each boron atom burned as are formed for each fission event, the values on the average-fissions-per-cubic-centimeter curve derived from irradiation data of uranium dioxide-stainless steel were divided by four to arrive at about the same gas pressure per unit volume. The allowable burnup between 230 and 427°C was obtained by extrapolation of the curves from both sides of this region.

D. Life of Filter

1. Design Limitations

The operating life of the filter must be determined in relation to the ETR core life to ensure that the filter life does not restrict the normal operation of the entire ETR facility. The operating life of the filter is restricted either by irradiation damage to filter material or by the change in flux or power gradient in the fuel element caused by burnup of the ^{10}B atoms of the filter. Table XI shows the probable limitations based on a boron stainless steel filter for these variables.

TABLE XI. Filter Design Limitations

	Design Limitation
Irradiation damage to filter	20% ^{10}B burnup
Fuel-element power	±15%
Power gradient in test assembly	1.5 max/min

2. Effect of Irradiation Damage on Filter Life

Figure 14 shows the neutron heating and ^{10}B burnup characteristics of the filter as a function of ^{10}B concentration in units of atoms/cm^2 of filter surface. The design is a stainless steel cylindrical filter containing 5.2×10^{21} ^{10}B atoms/cc of alloy. This is equivalent to 2.0×10^{21} atoms/cm^2 of the inside surface of the filter. At this concentration, the destruction rate of ^{10}B in the filter is 0.66% per day. The filter life was estimated by Atomic Power Development Associates[15] and is shown in Table XII. Sufficient cooling is supplied to remove the neutron heating of the ^{10}B and the gamma heating of the stainless steel in the filter.

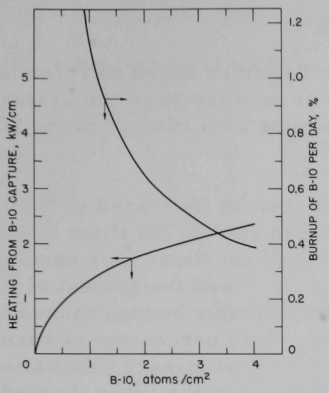

Fig. 14

Heating and Burnup Characteristics of Thermal-neutron Filter as a Function of ^{10}B Concentration

TABLE XII. Filter Life

Time, days	Filter Burnup, at. % ^{10}B	Power, kW/cm	Power Depression, max/min
0	0	0.65	1.31
20	12.5	0.68	1.37
40	25.0	0.71	1.44
60	37.5	0.75	1.52
80	50.0	0.79	1.63

Filter ^{10}B concentration, 2.0×10^{21} atoms/cm^2.
Enrichment, 47.5%.

Because of irradiation damage considerations, the filter is limited to 20% burnup of the ^{10}B atoms. A filter life of approximately 32 days can be expected before this burnup is exceeded.

3. Allowable Stress

In the unirradiated condition, the alloy of boron and stainless steel is sufficiently ductile to permit normal forming and machining procedures.

After an appreciable amount of burnup takes place, the boron-stainless steel alloy becomes brittle at irradiation temperatures of less than 250°C. Therefore, to preclude the possibility of cracking because of stresses during irradiation, the filter will be designed so that all deformation will be in the elastic range and so that the maximum allowable stress will be 25,000 psi. As determined from postirradiation tensile tests on irradiated material of approximately the same composition as the filter, this amount of stress is well within the allowable limits.

4. Allowable Filter Lifetime

Table XII compares filter lifetimes based on filter irradiation damage, fuel-element power, and power depression in the assembly. These data indicate that the filter life is adequate with respect to the ETR operating cycle.

The allowable filter burnup can be increased if (1) the concentration of the ^{10}B (atoms/cc) is decreased and (2) the filter thickness is increased to keep the product (atoms/cm^2) constant. For example, if the filter thickness is increased by a factor of 3 and the amount of ^{10}B is decreased to 0.0042×10^{24} atoms/cc, the allowable burnup caused by irradiation damage would be increased to 40%. This percentage of burnup is equivalent to a filter lifetime of 53 days. Preliminary calculations show that the increased temperature and stresses in the filter, caused by increased gamma heating and a thicker filter, is still within the design limitation. Temperatures and stresses are discussed in Section E below.

E. Filter Temperatures and Stresses

1. Power Generation

The filter power generation is about 300 kW. Assuming that two thirds of the heat generated is removed from the outer surface of the filter, the maximum heat flux is about 95 W/cm^2 sec.

The boron concentration in the filter is 2.0×10^{21} ^{10}B atoms/cm^2. Figure 14 shows that the maximum neutron-capture heating is about 2.4 kW/cm. From the data in IDO-16667,[18] the maximum gamma heating is estimated to be 2.4 kW/cm. Figure 15 shows the computed curve of heat-generation distribution in the filter wall at the location of maximum heating.

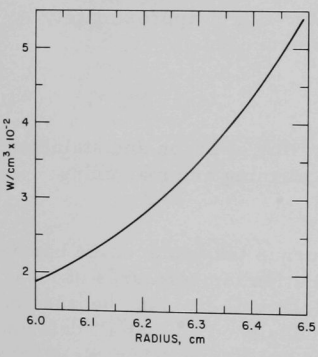

Fig. 15. Internal Heat Generation in Thermal-neutron Filter as a Function of Radius

2. Temperatures

The basic differential equation for temperature is

$$\frac{d^2T}{dR^2} + \frac{1}{R}\frac{dT}{dR} = -\frac{H(R)}{K},$$

where

T = temperature,

R = radius of filter,

K = thermal conductivity,

and

H(R) = heat-generation rate.

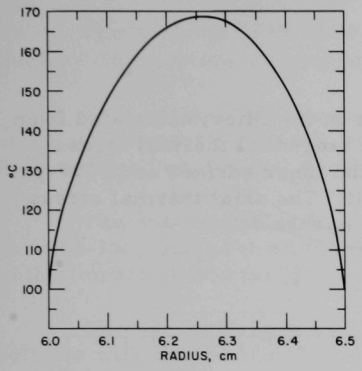

Fig. 16. Radial Temperature Distribution in the Filter

Figure 16 shows the temperature profile for the filter as calculated from the data of Fig. 15. Exact determination of the temperature distribution is made difficult by both the nonuniformity of the neutron-capture heat generation and by the uncertainties in the values for gamma heating.

The profile is hardly affected by a change in surface temperature; thus, the temperature gradient is independent of the coolant velocity. The maximum temperature in the filter is approximately 150°C for the sodium flowrate of 439 g/cm^2-sec.

3. Stresses

The thermal stresses in the filter are a result of the temperature gradients. The basic equations for the thermal stresses in a hollow cylinder, as taken from Theory of Elasticity,[19] are

$$\sigma_\theta = \frac{\alpha E}{1-\gamma}\frac{1}{R^2}\left[\frac{R^2+R_a^2}{R_b^2-R_a^2}\int_{R_a}^{R_b} TR\,dR - \int_{R_a}^{R} TR\,dR - TR^2\right]$$

$$\sigma_z = \frac{\alpha E}{1-\gamma}\left[\frac{2}{R_b^2-R_a^2}\int_{R_a}^{R_b} TR\,dR - T\right],$$

and

$$\sigma_\gamma = \frac{\alpha E}{1-\gamma}\frac{1}{R^2}\left(\frac{R^2-R_a^2}{R_b^2-R_a^2}\int_{R_a}^{R_b} TR\,dR - \int_{R_a}^{R} TR\,dR\right),$$

where

σ_θ = tangential stress,
σ_z = axial stress,
α = coefficient of thermal expansion,
E = modulus of elasticity,
γ = Poisson's ratio,
R = cylinder radius,

R_a = inside radius of filter,

R_b = outside radius of filter,

and

T = temperature.

Figures 17 and 18 show the thermal stresses in the filter, calculated from the temperature distribution in Fig. 16. The tangential thermal stress reaches a peak value of 9000-psi tension at the inner surface and 7000-psi compression near the center of the filter wall. The axial thermal stress peaks at 7000-psi tension and at 3500-psi compression.

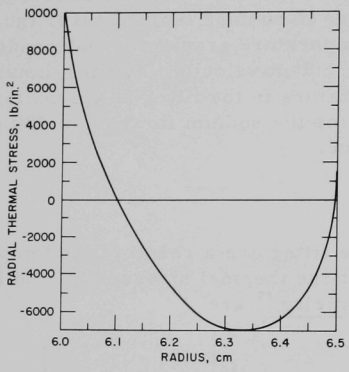

Fig. 17. Radial Thermal Stress in the Filter

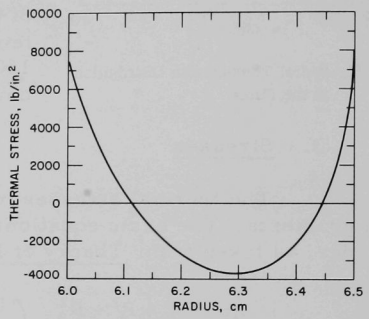

Fig. 18. Axial Thermal Stress in the Filter

If the filter can be considered a thin cylinder, the thermal stress will be only a function of the difference between the surface temperature and maximum temperature. Increasing the filter thickness increases the thermal stress. The temperature difference increases in nearly the same ratio as the thickness. Increasing the thickness increases the maximum thermal stress to approximately 15,000 psi, which is well within the design limit of 25,000 psi.

Proper design will hold these stresses to small values, so that the combined thermal and mechanical stress does not exceed 25,000 psi.

VII. SAFETY ANALYSIS

A. Analysis of Test Loop

The analysis of the test loop is the responsibility of both the Idaho Nuclear Corporation and Argonne National Laboratory.

This analysis will present an initial evaluation of the safety aspects of a Fuel Element Failure Propagation (FEFP) irradiation program for the ETR using a liquid-metal package-loop facility.

The analysis will include the present status of the safety-related package-loop design in sufficient detail to allow independent evaluations of the impact of this facility on the ETR and associated experiments.

The quality assurance and administrative control procedures and policies will also be included to provide reliability assurance for the safe design and operation of the facility.

B. Analysis of Test Assembly

The analysis of the test assembly is an aspect of safety analysis concerned with the period of time from the initiation of an accident to the failure of one fuel element. An objective of the FEFP program[20] is to investigate how the loss of structural integrity of one fuel element affects the other fuel elements in the assembly of elements that constitute the test specimen. Thus this is a program of planned accidents with the possibility of some unplanned ones, all of which must be contained within a test loop located in the J-13 space of ETR.

The time-dependent sodium pressure resulting from both planned and unplanned accidents will be the subject of a later analysis.

The analysis presented in this report concerns averting damage by possible unplanned accidents, such as a loss of filter or coolant.

The most obvious sources of unplanned accidents in this testing technique stem from the loss of filter effectiveness and the loss of sodium coolant. The filter effectiveness can be diminished by isotopic changes in filter materials, by melting, and by mechanical damage. The ability of the sodium to remove heat from the test fuel elements can be diminished by pump trouble, by sodium boiling, and by a break in the piping. Any accident, short of an instantaneous disintegration of the filter and loss of all sodium, will involve a period of time between the instant the filter and/or the coolant

effectiveness starts to diminish to the time the UO_2 melts, the sodium boils, and the stainless steel casing of the UO_2 melts or ruptures. The basis of this preliminary analysis is the relationship between the period of time from the initiation of trouble to the loss in structural integrity of the UO_2 casing and the period of time it takes to detect and control the trouble. The detection and control systems may prevent serious damage to the test loop and reactor if these systems can function before the casing of the UO_2 fails from other than indirect causes.

The intent is to try to estimate the periods of time involved in loss-of-filter accidents, loss-of-coolant accidents, and the highly improbable double accident of filter effectiveness and sodium flow decreasing at the same time.

The filter may lose its effectiveness while the coolant remains at full effectiveness, the coolant may lose its effectiveness while the filter remains at full effectiveness, or both filter and coolant effectiveness may diminish simultaneously. In any case, the result is the same: The temperatures and pressures in the test assembly will rise, and, unless some provision is made (such as concurrently lowering the power of the ETR), eventually the fuel casing will melt or rupture depending upon the relationship between the internal pressure, the metal temperature, and the ductility. The casing will stretch elastically until the yield stress is exceeded, and then it will stretch in accordance with the theory of plasticity until the ultimate stress is exceeded and rupture occurs. The maximum stress and the maximum casing temperature may not occur at the same axial position. The maximum stress is likely to occur near the longitudinal midpoint of the fuel element, where the UO_2 starts melting. The maximum casing temperature is likely to occur near the end of the fuel element, where the sodium starts to boil. The question is where the thermoelastic time relationship exists that will cause the fuel-element casing to fail in the shortest period of time after the filter starts to disintegrate and/or the coolant flow starts to decelerate. If there is no appreciable internal pressure, the casing will fail by melting near the end of the fuel element; if there is internal pressure due to expanding UO_2, the casing will fail by rupture near the midpoint; if there is internal pressure due to fission gas, the casing will fail near the hottest point. When the casing loses its structural integrity, the UO_2 and sodium can come into contact and a thermochemical reaction may occur and produce a rapid increase in sodium pressure.

The physical properties of irradiated stainless steel between 1000 and 1500°C are not precise. The melting point is around 1500°C. Also, the effect of molten UO_2 and boiling sodium on irradiated steel and the many variables in the transition from elastic to plastic phenomena cause uncertainty in the performance of the stainless steel casing in the range from 1000 to 1500°C.

We suggest that the criterion for the structural integrity of the casing be 1000°C. As long as the gap between the UO_2 and its casing is maintained at its present value and the tests on new fuel elements are of short duration, low contact and fission-gas pressures exist and the probability of exceeding the ultimate stress of the steel is low.

1. Filter

Because of the short duration of individual tests in the program, only mechanical damage and/or melting are likely to cause the filter to lose its effectiveness.

When all the fuel elements in an assembly of 19 are operating at the same power, the center fuel element must have a higher enrichment than fuel elements in the ring of six and fuel elements in the ring of six must have higher enrichment than fuel elements in the ring of 12. The tests are planned so that the total power in each fuel element is of the order of 45 kW. The average power that can be generated in a fuel element without melting UO_2 at the midpoint of the fuel element is calculated to be 60 kW.

The fuel elements are so designed that with the filter in place this value of 60 kW per fuel element is not exceeded if the test assembly is in the J-13 space and the ETR power does not exceed 175 MW. The filter is the equivalent of 35 mils of cadmium. If the filter effectiveness diminishes to zero at a rate for which it is impossible to compensate, the heating rate of the assembly increases by a factor of 2.62 and the power of the fuel elements increases by a factor of 3.2 in the ring of 12, by a factor of 1.7 in the ring of six, and by a factor of 1.4 in the center.

As soon as the fuel elements in the ring of 12 melt, their shielding effect upon the elements in the rings of six and one is removed and the elements in the ring of six melt faster than did those in the ring of 12. The center fuel element melts faster than did those in the ring of 6. This is a fuel-failure propagation phenomenon unique to this way of testing fast-reactor fuel elements or any assembly in which the enrichment varies inversely as the radius of the assembly. Figure 19 shows the distribution of power in a fuel element of each ring just before melting. If all the fuel elements are operating at 45 kW/element, they will all melt. The rates of melting increase as successive outer rings are removed.

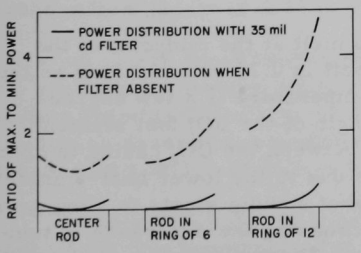

113-2553

Fig. 19. Distribution of Power in a Fuel Element with and without a Filter

2. Coolant

Since the characteristics of the fluid dynamics of the test loop are not known, the deceleration of sodium velocity (coastdown) is made a parameter. Figure 20 is a plot of velocity versus time. For example, if velocity decreases from 450 to 210 b/cm^2-sec when the power in the assembly is 60 kW/element, the sodium starts to boil in 2.17 sec. (Figure 20 was prepared by using the heat-transfer module of the SAS1A code.[13])

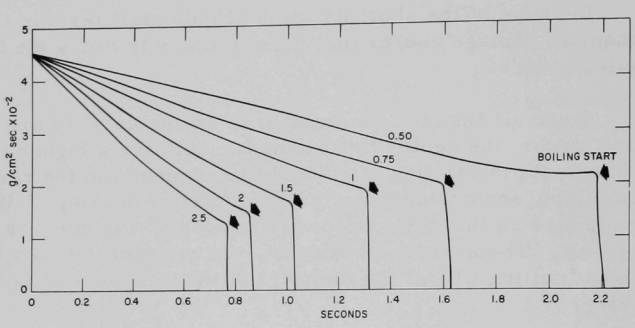

113-2552 Rev. 1

Fig. 20. Sodium Velocity vs Time with Flow Decay Constants vs Parameter

The following is a concept of an accident that might occur during a typical test: The total power in each element of the assembly of 19 is 45 kW. The average power density in each element is 2000 W/cm^3 of UO_2. Due to axial buckling, the maximum average power density over the cross section of a fuel element at its longitudinal midpoint is 2600 W/cm^3 of UO_2. The filter starts to disintegrate, and then its effectiveness becomes zero in 200 msec. The total power in an outer fuel element increases by a factor of 3.21 in 200 msec. At the instant the filter starts to disintegrate, the sodium velocity starts to decelerate following curve 1 on Fig. 20.

The result is that UO_2 starts to melt at the midpoint of the element in 0.6 sec. The sodium starts to boil in 0.79 sec. As long as the sodium is in the liquid phase, the casing temperature is a few degrees above the sodium temperature along the length of the UO_2 fuel element. When sodium starts to boil, the difference between the UO_2 casing temperature and the sodium temperature increases due to the lower heat-transfer rate of a vapor-liquid mixture, and the flow of sodium starts to slow down from its normal rate of 439 g/cm^2, thus increasing the difference in temperature between the casing and the sodium. The temperature of the boiling sodium remains constant, but the temperature of the casing increases as the percent vapor increases. The maximum casing temperature occurs near the end of the element. The casing temperature reaches 1000°C in 0.77 sec and its melting point of 1500°C in 1.23 sec.

The stress in the casing is negligible, since the gap between the UO_2 and the casing is such by design that as the temperature of both increase, their relative expansions do not result in any appreciable contact pressure being exerted on the casing. For a smaller gap and/or the presence of fission gas, this internal pressure can be appreciable. These test elements have not been exposed to any appreciable radiation.

C. Possible Accident Conditions

Since the higher the power at which the elements are operating when an accident occurs the shorter the period of time until the casing loses its structural integrity, the following five hypothesized accidents are initiated when the fuel elements are operating at 60 kW per element:

1. The filter is disintegrating from full effectiveness to zero in 0.2 sec, and the sodium pump is running at full power. The fuel element is in the ring of 12 in an assembly of 19 fuel elements, and power in the fuel element increases by a factor of 3.21 in 0.2 sec.

2. The filter is disintegrating from full effectiveness to zero in 0.1 sec, and the sodium pump is running at full power. The fuel element is in the ring of 12 in an assembly of 19 fuel elements, and power in the fuel element increases by a factor of 3.21 in 0.1 sec.

3. The filter remains intact, and the sodium pump stops. The sodium velocity is shown by curve 1 of Fig. 20. The fuel element is in the ring of 12 in an assembly of 19 fuel elements, and power in the fuel element remains constant.

4. The filter is disintegrating from full effectiveness to zero in 0.2 sec, and the sodium pump stops at the instant the filter starts to go. The sodium velocity follows curve 1 of Fig. 20. The fuel element is in the ring of 12 in an assembly of 19 fuel elements, and power in the fuel element increases by a factor of 3.21 in 0.2 sec.

5. The filter is disintegrating from full effectiveness to zero in 0.1 sec, and the sodium pump stops at the instant the filter starts to go. The sodium velocity follows curve 1 of Fig. 20. The fuel element is in the ring of 12 in an assembly of 19 fuel elements, and power in the fuel element increases by a factor of 3.21 in 0.1 sec.

Table XIII lists the thermodynamic conditions prevailing during each of the five hypothesized accidents.

TABLE XIII. Thermodynamic Conditions during Hypothesized Accidents

Hypothesized Accident No.:	1	2	3	4	5
Total power in fuel element at time zero, kW	60	60	60	60	60
Average power density at center of fuel element at time zero, W/cm^3 of UO_2	3900	3900	3900	3900	3900
Sodium flow at time zero, g/cm^2-sec	439	439	439	439	439
Sodium inlet temperature, °C	500	500	500	500	500
Maximum UO_2 temperature, °C	3091	3112	2605	3004	3008
Time until UO_2 starts to melt, sec	0.400	0.385	3.643	0.309	0.380
Time until sodium starts to boil, sec	0.629	0.578	2.168	0.545	0.504
Time until casing reaches 1000°C, sec	0.525	0.495	2.030	0.487	0.465
Time until casing reaches 1500°C, sec	1.016	0.899	3.648	0.845	0.725
Stress at hottest spot of casing, $dynes/cm^2$	Negl.	Negl.	Negl.	Negl.	Negl.
Maximum stress in casing, $dynes/cm^2$	Negl.	Negl.	Negl.	Negl.	Negl.
Distance of maximum stress from inlet end of fuel element, cm	-	-	-	-	-

D. Effect of Filter Loss upon Reactivity of ETR

The experiments planned for the ETR include up to 19 UO_2 fuel elements surrounded by a neutron filter designed to remove low-energy neutrons. The materials and location of this filter will be chosen to reduce the possibility of loss to an acceptably low value. Since the possibility cannot be completely eliminated, Idaho Nuclear Corporation will analyze the reactivity effect of such a loss on the ETR.

The accident model assumes the filter fails in 200 msec. This represented a conservative value with respect to melt-slumping mechanisms or mechanical loss.

The power trip level for ETR scram is 210 MW, and the scram delay is 20 msec. The total reactivity is 6.62 dollars, the fuel expansion coefficient is 0.00147 dollar/°F, and the moderator coefficient is 0.02649 dollar/°F.

E. Conclusions

1. The physical properties of UO_2, CdO, boron, and stainless steel at high temperatures and the concurrent phenomena of melting UO_2 and boiling sodium are encumbered with uncertainties and lack of experimental verification. It is therefore concluded that the casing may lose its structural integrity whenever thermoelastic conditions are concomitant with a rise in casing temperature from 1000 to 1500°C (the melting point of stainless steel).

The stainless steel casing of the fuel element reaches 1000°C in 0.465 sec for the conditions of the improbable double accident (hypothesized accident No. 5). The estimated time to detect trouble and scram the ETR is 0.260 sec. Since the melting point of the filter material is above 1500°C, and since the structural integrity of the filter is enhanced by its stainless steel casing, the probability of losing a filter is very low. In the event of this highly improbable double accident (hypothesized accidents, 4 and 5), the time required for the casing to reach 1000°C is 1.72 times as long as the period of time required to detect the trouble and scram the ETR. The period of time for the casing to reach 1500°C is 2.68 times as long as the period of the estimated time required to detect the trouble and scram the ETR.

2. The time required for a melting filter to be removed from the test section is estimated to be 0.2 sec. If this should actually be 0.1 sec, time for the casing temperature to reach 1000°C would be reduced by 0.03 sec. This change is largely due to the low thermal conductivity of UO_2.

3. The size of the gap between the UO_2 and the inside surface of the stainless steel casing determines what stress will exist, provided the fuel elements are not in the reactor long enough to build up fission-gas pressure. In these experiments, the gap is wide enough not to cause any appreciable stress, the fuel elements are all new, and the tests are of such duration that no fission-gas pressure occurs.

VIII. SHUTDOWN TEMPERATURE LIMITATIONS

A. Allowable Postirradiation Temperatures

At any time after normal in-pile loop operation, the temperature of the individual fuel elements resulting from decay heating of the fuel must be limited to prevent postirradiation changes in the metallurgical properties of the fuel. If excessive temperatures occurred after irradiation, the resultant changes in the properties of the fuel element might be indistinguishable from the irradiation effects.

To estimate the maximum allowable temperature after shutdown for metallic, cermet, and ceramic fuel elements, data from postirradiation heating of the various elements should be examined. This examination would indicate what surface temperature would be allowable for UO_2 fuel. At these temperatures, the creep properties of the materials begin to decrease, and swelling may occur because of fission-gas pressure. The use of surface temperature instead of central temperature is permissible, since the temperature drop in the individual fuel elements is small after a decay time of one day.

A maximum allowable shutdown temperature of 700°C is suggested.

B. Decay-heat Generation[15]

The decay-heat generation from a test assembly is a function of the following factors:

1. Residence time of the test assembly in the reactor.
2. Operating power of the test assembly.
3. Time since reactor shutdown (decay time).

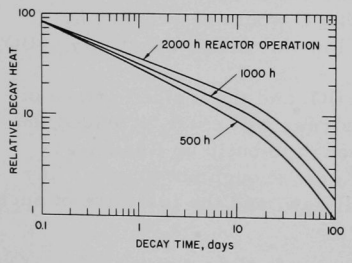

Fig. 21. Decay Heat of Seven-fuel-element Test Assembly

Relative decay-heat generation was calculated for several reactor residence times using the method employed by Perkins.[21] The results of these calculations are shown in Fig. 21.[15]

If the coolant pump and the heat exchanger are operated after the reactor is shut down, the maximum fuel-element surface temperature will be approximately 700°C, irrespective of decay time. The most severe heat-transfer conditions

occur if the sodium coolant is drained from the fuel assembly and if stagnant helium surrounds the elements within the fuel assembly. Heat-transfer calculations show that the fuel surface temperature will exceed 700°C in less than 1 min. For this reason, the fuel assembly must be immersed in sodium during all out-of-pile operations after irradiation.

If the coolant pump is shut down after the reactor is shut down, the surface temperature of the fuel assembly will rise to an equilibrium temperature which is dependent on the decay-heat generation and the thermal-resistance characteristics of the loop walls and helium annuli. Heat-transfer calculations have been made to determine the equilibrium fuel surface temperature after 2000 hr of reactor operation before shutdown. Calculations were performed with the loop immersed in water (natural convection) and with the loop in an air environment (forced convection). The results of these calculations are shown in Fig. 22.[15]

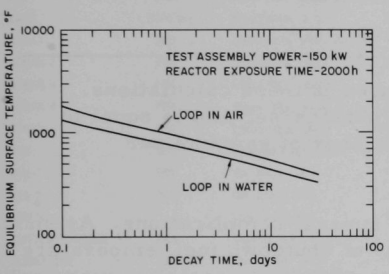

Fig. 22. Surface Temperature of Elements in a Seven-fuel-element Assembly

C. Minimum Decay Time

The curves in Fig. 22 indicate that once the reactor has been shut down the pumps and the heat exchanger must operate for about 8 hr to ensure that the maximum surface temperature of 7000°C is not exceeded for the cermet and ceramic fuel elements. An additional 16 hr decay in water is needed before the loop may be removed from the water and exposed to air.

IX. LOOP HANDLING

Removal of the loop from the reactor vessel is necessary at appropriate intervals for inspection and maintenance of the loop and the test assembly. Replacement of the thermal-neutron filter and the fuel element will be required at approximately 2-month intervals.

The most significant factors involved in handling the loop are the size and weight of the loop, the radioactivity of loop components, the fuel-element decay heat, the reactivity of the sodium with air and water, and the requirement to keep the loop in a position not more than 30° from the vertical position. APDA estimated the source strengths of the sodium contained within the loop, fuel, and stainless steel components. These are presented here in Table XIV to indicate order of magnitude. All shielding requirements for loop handling and hot-cell operations have been based on these calculations.

TABLE XIV. Source Strengths of Loop Components[a]

Decay Time	Sodium Gamma Curies[b]	Fuel-specimen Gamma Curies[b]	Stainless Steel Gamma Curies[b]
0	1.21×10^4		
1 hr	1.16×10^4		
2.4 hr		1.63×10^5	1.25×10^3
1 day	3.99×10^3	9.3×10^4	1.18×10^3
1 week	5.14×10^0	5.33×10^4	
1 month	5.61×10^{-2}	2.48×10^4	

[a] A reactor exposure of 10,000 hr was used in these calculations.
[b] One gamma curie = 3.7×10^{10} gamma-photons/sec and is equal to the actual curie value divided by the number of gammas per disintegration.

The decay-heat problem presents several complications. As shown in Section VIII.C, preliminary calculations of shutdown fuel temperature indicate that whether or not the fuel can be adequately cooled is marginal, unless the decay heat is removed by forced cooling for about one day after reactor shutdown. Therefore, the handling procedures described here are based on keeping the loop in operation inside the reactor vessel for one day after reactor shutdown before attempting loop-transfer operations. This requirement may complicate reactor operating procedures; therefore, a more detailed study should be made of the decay-heat problem to ascertain whether the delay occasioned by the necessity for cooling the loop after shutdown can be avoided.

The size of the loop as finally designed will determine the method of removing the loop from the reactor.

Emergency conditions that might arise during loop transfer operations and the methods of coping with these situations must be analyzed in detail.

APPENDIX A

A List of the Test and Experimental Reactors in the U.S.A.

	Date of Criticality	Location	Type	Output	Maximum Thermal Flux, n/cm^2-sec
AARR	1971	Argonne, Ill.	Tank, 93% U, H_2O	100 MW	5×10^{15}
AE-6	1952/1956	Santa Susana, Cal.	Aqueous homogeneous, 93% U, H_2O	2 kW	8×10^{10}
AFSR	1959	Argonne, Ill.	Fast, 90% U, air	1 kW	Fast 6×10^{11}
AGN-211-103	1959	Morgantown, W. Va.	Solid homogeneous, 20% U, polyethylene	75 W	3×10^{9}
ALRR	1964	Ames, Iowa	Tank, 94% U, H_2O	5 MW	10^{14}
ARGONAUT	1957	Argonne, Ill.	Argonaut, 20% U, graphite, water	10 kW	1.7×10^{11}
ARR	1956	Chicago, Ill.	Aqueous homogeneous, 88% U, H_2O	100 kW	2×10^{12}
ATR	1968	Idaho Falls, Idaho	Tank, 93% U, H_2O	250 MW	10^{15}
BGRR	1950/1958	Brookhaven, N.Y.	93% U, graphite, air	20 MW	10^{13}
BORAX-1	1953	Idaho Falls, Idaho	Tank, 90% U, H_2O	Destroyed 1954	
BORAX-2	1954	Idaho Falls, Idaho	Tank, 90% U, H_2O	Shut down 1958	
BORAX-3	1955	Idaho Falls, Idaho	Tank, 90% U, H_2O	Shut down 1956	
BORAX-4	1956	Idaho Falls, Idaho	Tank, 90% U-Th, H_2O	Shut down 1958	
BORAX-5	1962	Idaho Falls, Idaho	Tank, 90% U, H_2O	Shut down 1964	
BRR	1956	West Jefferson, Ohio	Pool, 90% U, H_2O	2 MW	1.8×10^{13}
BSR-1	1950	Oak Ridge, Tenn.	Pool, 93% U, H_2O	1 MW	10^{13}
BSR-2	1959	Oak Ridge, Tenn.	Pool, 93% U, H_2O	750 kW	10^{13}
BAWTR		Lynchburg, Va.	Pool, H_2O	6 MW	1.2×10^{14}
BUFFALO REACTOR	1961	Buffalo, N.Y.	Pool, 90% U, H_2O	1 MW	10^{13}
CLEMENTINE	1946	Los Alamos, N.M.	Fast, Pu, Hg	25 kW	Fast 5×10^{12}
CP-1	1942	Chicago, Ill.	Natural U, graphite	200 W	4×10^{6}
CP-5	1954	Argonne, Ill.	Tank, 90% U, D_2O	5 MW	10^{14}
CWRR	1958	Quehanna, Pa.	Pool, 93% U, H_2O	Shut down 1966	
EBOR	1964	Idaho Falls, Idaho	Solid homogeneous, 62.5% U, BeO, He	Terminated 1966	
EBR-I	1951	Idaho Falls, Idaho	Fast, Pu, NaK	Shut down 1964	
EBR-II	1963	Idaho Falls, Idaho	Fast, Pu, Na	62.5 MW	
EBWR	1956	Argonne, Ill.	Tank, U, H_2O	Shut down 1967	
ESADA-VESR	1963	Pleasanton, Cal.	Tank, 5.4% U, H_2O	Shut down 1967	
ETR	1957	Idaho Falls, Idaho	Tank, 93% U, H_2O	175 MW	5×10^{14}
FFTF	1973	Richland, Wash.	Fast, U-Pu, Na	400 MW	10^{15}
FNR	1957	Ann Arbor, Mich.	Pool, 90% U, H_2O	1 MW	1.4×10^{13}
GETR	1958	Pleasanton, Cal.	Tank, 90% U, H_2O	50 MW	2×10^{14}
HEW-305	1945	Richland, Wash.	Natural U, graphite	30 W	1.35×10^{7}
HFBR	1965	Brookhaven, N.Y.	Tank, 90% U, D_2O	40 MW	7×10^{14}
HFIR	1965	Oak Ridge, Tenn.	Tank, 93% U, H_2O	100 MW	5×10^{15}
HHLR	1960	Watertown, Mass.	Pool, 93% U, H_2O	1 MW	10^{13}
HPRR	1963	Oak Ridge, Tenn.	Fast, 93% U	1 kW	Fast 1.5×10^{9}
HRE-1	1952	Oak Ridge, Tenn.	Aqueous homogeneous, 93% U, H_2O, D_2O refl.	Shut down 1954	
HRE-2	1957	Oak Ridge, Tenn.	Aqueous homogeneous, 93% U, D_2O	Shut down 1961	
HWCTR	1962	Aiken, S.C.	Tank, 93% U, D_2O	Shut down 1964	
HYPO	1944	Los Alamos, N.M.	Aqueous homogeneous, 14.5% U, H_2O	6 kW	1.9×10^{11}
IRL	1959	Plainsboro, N.J.	Pool, 90% U, H_2O	1 MW	7×10^{13}
ISU-UTR-10	1959	Ames, Iowa	Argonaut, 92% U, graphite, H_2O	10 kW	1.3×10^{11}
JUGGERNAUT	1962	Argonne, Ill.	Argonaut, 93% U, graphite, H_2O	250 kW	4×10^{12}
KEWB	1956	Santa Susana, Cal.	Aqueous homogeneous, 93% U, H_2O	50 kW	7×10^{11}
L-77	1958	Los Angeles, Cal.	Aqueous homogeneous, 20% U, H_2O	10 W	2.5×10^{8}
LAMPRE	1959	Los Alamos, N.M.	Fast, Pu, Na	Shut down 1963	
LAPRE-1	1956	Los Alamos, N.M.	Aqueous homogeneous, 93% U, H_2O + H_3PO_4	Shut down 1957	
LAPRE-2	1959	Los Alamos, N.M.	Aqueous homogeneous, 93% U, H_2O + H_3PO_4	Shut down 1959	

	Date of Criticality	Location	Type	Output	Maximum Thermal Flux, n/cm^2-sec
LITR	1950	Oak Ridge, Tenn.	Tank, 30% U, H_2O	3 MW	3.5×10^{13}
LOFT	(1970)	Idaho Falls, Idaho	Tank, H_2O	50 MW	
LOPO	1944	Los Alamos, N.M.	Aqueous homogeneous, 15% U, H_2O	0.01 W	Not available
LPR	1958	Lynchburg, Va.	Pool, 90% U, H_2O	1 MW	4.3×10^{13}
LPTR	1957	Livermore, Cal.	Pool, 93% U, H_2O	2 MW	5×10^{13}
MITR	1958	Cambridge, Mass.	Tank, 90% U, D_2O	2 MW	4.7×10^{13}
MRR	1959	Upton, N.Y.	Tank, 90% U, D_2O	5 MW	
MSRE	1964	Oak Ridge, Tenn.	93% U, graphite, molten salt	10 MW	8.4×10^{13}
MTR	1952	Idaho Falls, Idaho	Tank, 93% U, H_2O	40 MW	4.8×10^{14}
NASA-MUR	1964	Sandusky, Ohio	Tank, 93% U, H_2O	100 kW	5×10^{11}
NASA-TR	1961	Sandusky, Ohio	Tank, 93% U, H_2O	60 MW	3×10^{14}
NBSR	1965	Gaithersburg, Md.	Tank, 90% U, H_2O	10 kW	10^{14}
NCSCR-3	1960	Raleigh, N.C.	Pool, 90% U, H_2O	10 kW	1.5×10^{11}
NSR	1958	Upton, N.Y.	Tank, 90% U, H_2O	100 kW	5×10^{10}
NTR	1957	Pleasanton, Cal.	Tank, 90% U, H_2O	30 kW	9×10^{11}
OMRE	1957	Idaho Falls, Idaho	Natural U, organic moderator	Shut down 1963	
ORR	1958	Oak Ridge, Tenn.	Tank, 90% U, H_2O	30 MW	4×10^{14}
OWR	1956	Los Alamos, N.M.	Tank, 95% U, H_2O	8 MW	
PBF	(1970)	Idaho Falls, Idaho	Tank	20 MW	
PCTR	1955	Richland, Wash.	90% U, graphite	10-100 W	10^{9}
PDP	1953	Aiken, S.C.	Tank, variable fuel, D_2O	1 kW	10^{8}
PR	1959	Pawling, N.Y.	Tank, 92.5% U, D_2O	5 W	2×10^{8}
PRPR	1960	Mayaguez, P.R.	Pool, 20% U, H_2O	1 MW	5×10^{12}
PRR	1959	Mayaguez, P.R.	Aqueous homogeneous, 20% U, H_2O	10 W	2.5×10^{8}
PRTR	1960	Richland, Wash.	Tank, Pu + U, D_2O	120 MW	10^{14}
PSR	1955	Pennsylvania	Pool, 93% U, H_2O	200 kW	3.5×10^{12}
RSCW	1961	Pullman, Wash.	Pool, 90% U, H_2O	100 kW	1.1×10^{12}
SER		Sandia Base, N.M.	Tank	5 MW	
SP	1953	Aiken, S.C.	Tank, 90% U, H_2O	10 MW	3×10^{11}
SPERT-1	1955	Idaho Falls, Idaho	Pool, 93% U, H_2O	Shut down 1964	
SPERT-2	1959	Idaho Falls, Idaho	Tank, 93% U, H_2O or D_2O	Shut down 1965	
SPERT-3	1958	Idaho Falls, Idaho	Tank, 94% U, H_2O	60 MW Transient	6×10^{14}
SEFOR	1968	Strickler, Ark.	Fast, U-Pu, Na	20 MWt	
SRE	1957	Santa Susana, Cal.	Tank, Graph, Na	Shut down 1966	
SPERT-4	1962	Idaho Falls, Idaho	Pool, 93% U, H_2O	Transient	
SPR	1959	Stanford, Cal.	Pool, 94% U, H_2O	10 kW	10^{11}
SPR	1961	Sandia Base, N.M.	Transient	Shut down 1967	
SR-305	1952	Aiken, S.C.	Natural U, graphite	25 W	2×10^{7}
SUPO	1944/1951	Los Alamos, N.M.	Aqueous Homogeneous, 89% U, H_2O	25 kW	1.2×10^{12}
TREAT	1959	Idaho Falls, Idaho	Solid Homogeneous, 93% U, graphite, air	1000 MW-sec	2×10^{16}
TRIGA	1958	San Diego, Cal.	Solid Homogeneous, 20% U, ZrH + H_2O	250 kW	10^{13}
TRR	1951	Richland, Wash.	Tank, 93% U, H_2O	100 W	3.3×10^{9}
UCC-ND	1961	Sterling Forest, N.Y.	Pool	5 MW	
UCNCR	1961	Tuxedo, N.Y.	Pool, 93% U, H_2O	5 MW	10^{14}
UFTR	1959	Gainsville, Fla.	Argonaut, 20% U, graphite, H_2O	10 kW	10^{11}
UHTREX	1967	Los Alamos, N.M.	93% U, graphite, He	3 MW	5.5×10^{13}
UTR-1	1958	Mountain View, Cal.	Argonaut, 93% U, graphite, H_2O	1 W	10^{7}
UVAR	1960	Charlottesville, Va.	Pool, 20% U, H_2O	1 MW	2.6×10^{13}
UWNR	1961	Madison, Wis.	Pool, 90% U, H_2O	10 kW	10^{11}
UWRR	1959	Laramie, Wyo.	Aqueous homogeneous, 20-90% U, H_2O	10 W	2.5×10^{8}
VBWR	1957	Pleasanton, Cal.	Tank, H_2O	Shut down 1963	
VPI-UTR-10	1959	Blacksburg, Va.	Argonaut, 90% U, H_2O	10 kW	1.5×10^{11}
WPIR	1959	Worcester, Mass.	Pool, 90% U, H_2O	1 kW	9×10^{9}
WTR	1959	Waltz Mill, Pa.	Tank, 93% U, H_2O	Shut down 1962[a]	
X-10	1943	Oak Ridge, Tenn.	Natural U, graphite, air	3.5 MW	1.1×10^{12}

[a]Reactivated 1968.

APPENDIX B

Possible Reactors for FEFP Program

1. Advanced Test Reactor (ATR)

The ATR is owned by the AEC and will be operated by Idaho Nuclear Corporation. The reactor is presently being tested and should be ready for operation in 1970. This reactor has nine in-core loop positions, each 5.25 in. in diameter. At a reactor power of 250 MWt, the fast flux in these test holes is 15×10^{14} nv. Furthermore, the core height is 49.5 in. The ATR could accommodate a 5-in.-diam concentric loop design, and most of the thermal flux could be masked out to obtain a high epithermal flux.

The license would have to be changed for the installation of a sodium loop, and the sodium/water safety analysis would have to be made. The absence of water in the test thimbles is a safety advantage, but poses additional problems on heat removal from the sodium and neutron shield. Scheduling our experiments not to conflict with other users is uncertain, since complete schedules have not been developed at this time. The reactor has been designed to accommodate loops, and there should be little interference with overhead operating mechanisms in the reactor. The control rods are driven from the bottom by a horizontal drive rod.

The ATR is heavily committed to U.S. Navy reactor testing program, and consequently scheduling and availability will probably be difficult. The power level would be controlled by the principal user, and the flexibility required for our experiments may not be attainable.

2. Babcock and Wilcox Test Reactor (BAWTR)

Pool-type reactors make up almost half of a list of experimental and test reactors. Most of these are low-power training reactors constructed by universities to assist in teaching nuclear courses. The analysis of the BAWTR shows that, even at 6 MW, there is insufficient epithermal flux to obtain 20 kW/ft in our test elements. This type of reactor must essentially be rebuilt to a power of about 20 MW and an average power density of 400 kW/liter in the core. More than a million dollars would be needed for this modification.

The BAWTR is owned and operated by the Babcock and Wilcox Company. The reactor has a low flux (3×10^{13} nv), a large research facility (6 by 6 in.), and a good core height (30 in.). According to the B&W analysis, even the 1.2×10^{14} thermal flux produces only 18 kW/ft in the test element. To raise the reactor power rating to 20 MW, a major redesign of the reactor would be necessary, including pressurization, at considerable cost, perhaps several million dollars. The attendant increase by a factor of about three in specific power would still be insufficient for the tests in this program.

Possibly, a modified Mark-II loop could be accommodated in a 6- by 6-in. hole in BAWTR, since there is a 4-in. hole in the lower grid plate and a 3-ft clearance beneath the plate. Considerable rearrangement of the reactor control units would be necessary (and difficult). The test section in such a rearrangement would probably be off center by several inches. Such modification would result in essentially a new core and would require considerable physics and hazards analyses.

The BAWTR, operating at 6 MW, provides only a fraction of the required power density (even with full sample enrichment) for reasonably uniform specific power-density distributions through and among elements.

3. Engineering Test Reactor (ETR)

The ETR is owned by the AEC and operated by Idaho Nuclear Corporation. The reactor has been used for research and isotope production since 1958. The active core height is 3 ft, and there are nine high-flux test holes suitable for loop installation. These test facilities vary in size from 3 to 9 in. square. The reactor power is 175 MW, and a fast flux of 3×10^{14} nv is available in the test facilities. The ETR can easily accommodate all the tests contemplated in our program. With reasonable masking and enrichment, preliminary uniformity estimates by Idaho Nuclear indicate a 3% variation in fission densities across pins and a 10% variation across a subassembly.

A change in license either would not be needed or would be obtained readily, since Pratt and Whitney has already installed a sodium loop in the ETR. In addition, the sodium/water reactions have been assessed. The control-rod drive mechanisms are located below the core and would not interfere with a loop installation. There appears to be ample space above the reactor for loop auxiliary equipment.

The principal problems in the use of this reactor are the conflict with other users and the availability of the test facilities when needed. Scheduling of experiments may impose serious limits on the number of experiments that can be performed in a reasonable length of time. If a test were scheduled at the end of each six-week reactor cycle, about six to eight experiments could be performed in a year. This number seems adequate for the first year's testing, if the amount of analysis and the number of posttest examinations are considered. In subsequent years, as the principal user moves his tests to the ATR, more failure-propagation tests can be scheduled. If scheduling and availability problems can be worked out, the ATR represents one of the best facilities for our experiments.

4. General Electric Test Reactor (GETR)

The GETR is a tank-type, 30-MW, materials-testing reactor, owned and operated by General Electric Company. The thermal flux (2×10^{14} nv)

and fast flux (5×10^{14} nv) are both high; the core height is 3 ft; but the available high-flux research modules are only 3 in. square--a minimum value. The control-rod drive is at the bottom of the reactor, where the control rod will not interfere with a loop installation. The handling of liquid-metal capsules (but not loops) and a power increase to 50 MW were recently approved for GETR by the AEC Division of Reactor Licensing.

At 50 MW, the GETR can produce high specific powers in test samples, even with the required masking of the low-energy neutron flux. Preliminary estimates made for a 1/4-in. pin having a fuel diameter of 0.22 in., and a 25% PuO_2-75% UO_2 composition in an off-center thimble indicate that the specific peak-power generation rate obtainable with a flux filter varies from 12 kW/ft at 20% ^{235}U enrichment to about 20 kW/ft at 90% ^{235}U enrichment. Estimated average power ratios among pins in a seven-pin cluster in this off-center core position run from 0.9 to 1.15 times average peak power for the optimum cluster orientation, and from 0.86 to 1.20 times average peak power for the most unfavorable orientation. These could be balanced by varying the enrichment among pins. Information is not available on variation within a pin, but it should not be more than about 3% with the flux filter.

A loop of the TREAT Mark-I type could be developed to fit in a 3-in.-square hole. Further investigation might show that some of our tests on seven-pin clusters could be conducted in this loop. Facilities exist such that test assembly and disassembly examinations can be conducted.

Preliminary investigations indicate the GETR will need extensive revisions to accommodate a sodium-cooled loop of the power and pressure rating and size required by the program.

5. Materials Testing Reactor (MTR)

The MTR is owned by the AEC and operated by the Idaho Nuclear Corporation. The reactor has been used for testing and research since 1952 and is not presently available. It has many positions for neutron irradiation but no in-core facilities. The core is only 2 ft high. At 40 MWt, the maximum flux in the core is 4.8×10^{14} nv thermal and 5.3×10^{14} nv fast. In the present reflector positions, the thermal flux is 3×10^{14} nv, but the fast flux is only 5×10^{14} nv.

The existing test holes in the reflector are too small (2 in.) and have a maximum fast flux of only 5×10^{13} nv. To produce the flux necessary for our tests, one or several fuel elements (each about 3 in. square) will have to be moved from the center of the core to reflector positions. Then, a fast flux of perhaps 5×10^{14} nv could be attained in the test facility, and either a concentric loop or a hairpin loop installed. Perhaps the Mark-I and Mark-II TREAT loops can be modified for this service. The control-rod drive mechanism is at the top of the reactor, and any loop installation will have to be designed around it.

The MTR is an attractive facility from the standpoint of scheduling and availability. However, the economic burden of operating the reactor solely for the FEFP program may prove to be too great. In addition, the core will have to be modified to provide both the flux and the large research hole needed for our tests. Some meltdown feasibility calculations and sodium/water hazards analyses have already been made. However, the cost of using and altering this reactor is too high. The MTR should only be considered further if no other reactor is suitable.

6. Transient Reactor Test (TREAT)

The TREAT facility represents the class of transient test reactors that could be considered for fuel-element failure-propagation tests. Other transient reactors are not suited for installing a sodium loop. The Power Burst Facility (PBF) is being built, and startup is expected in 1970. If available, the large central test thimble in the PBF could be used for some of these tests.

The TREAT facility is owned by the AEC and has been operated by Argonne National Laboratory since 1959. It has a 4-ft core, a maximum thermal flux of 20×10^{15} nv, and transient reactor power of 1000 MW. A central 4-in.-square test hole is normally used in the core, but additional fuel elements can be removed for larger test equipment.

The TREAT Mark-I and -II loops have been used successfully in this facility as a part of the Fuel Meltdown Program. In addition, a large recirculating sodium loop, in which low-pressure failure tests could be run, is completed and operational. It may be necessary to increase the thickness of the pressure tube wall to obtain the same rating as the Mark-II loop.

Tests in the Fuel Meltdown Program have demonstrated that TREAT can provide adequate fluxes for uniform or distributed fission rates. Suitable combinations of flux filters, absorbers, and enrichment variations were used in these tests. When the reactor power is 2000 MW and the automatic control system is installed, full power densities in the samples for several seconds may be realized. Running failure propagation tests in this short a time does not seem possible.

ACKNOWLEDGMENTS

The figures in Sections VI and VIII are based on work done in preparing Ref. 15 and presented here by courtesy of Atomic Power Development Associates.

REFERENCES

1. *Conceptual System Design Description for the LMFBR Fuel Element Failure Propagation Loop* (internal prepared by Argonne National Laboratory and Idaho Nuclear Corporation), 1969.
2. J. C. Carter, "Fast Reactor Fuel Testing in a Thermal Reactor," *Reactor Physics Division Annual Report: July 1, 1967 to June 30, 1968*, Paper IV-23, pp. 313-316 (Jan 1969).
3. E. E. Burdick, E. Fast, and D. W. Knight, *The Advanced Reactivity Measurement Facility*, IDO-17005 (1964).
4. *Engineering Test Reactor*, Idaho Nuclear Corporation; and *Fundamentals in the Operation of Nuclear Test Reactors, Vol. 3. Engineering Test Reactor Design and Operation*, IDO-1687-3 (July 1964).
5. G. J. Duffy, H. Greenspan, S. D. Sparck, J. V. Zapatka, and M. K. Butler, *SNARG-1D, A One-dimensional, Discrete-ordinate, Transport-theory Program for the CDC-3600*, ANL-7221 (June 1966).
6. Argonne Cross-section Set 201.
7. B. J. Toppel (Ed.), *The Argonne Reactor Computation (ARC) System*, ANL-7332 (Nov 1967).
8. Argonne Cross-section Set 345.
9. Private ANL memorandum from M. O. Davis.
10. R. E. Woods, J. F. Kunze, F. L. Sims, and C. S. Robertson, Jr., *A Filter for Fast Flux Testing in a Thermal Test Reactor*, Nucl. Appl. 5(3) (1968).
11. A. E. McArthy, *Gamma-ray Heating in an Assembly of Fast Reactor Fuel Elements Irradiated in the Center of the ETR Core*, unpublished ANL memo (Nov. 13, 1968).
12. T. Rockwell III (Ed.), *Reactor Shielding Design Manual*, TID-7004, 365 (1956).
13. D. R. MacFarlane, *SAS1A, A Computer Code for the Analysis of Fast Reactor Power and Flow and Transients*, ANL-7607 (to be published).
14. C. A. Hampel (Ed.), *Rare Metals Handbook*, Second Edition, Reinhold Publishing Corporation, New York (1961).
15. W. G. Blessing, *Conceptual Design of an In-Pile Package Loop for Fast Reactor Fuel Testing*, APDA-144 (July 28, 1961).
16. *Fast Reactor Core Design Parameter Study*, APDA-133 (March 1960).
17. *Symposium on Reactor Control Materials*, Nucl. Sci. Eng., Vol. 4, No. 3 (Sept 1958).
18. D. R. deBoisblanc *et al.*, *The Advanced Test Reactor-ATR Final Conceptual Design*, IDO-16667 (Sept. 20, 1960).
19. S. Timoshenko and J. N. Goodier, *Theory of Elasticity*, McGraw-Hill, 2nd Edition (1961).
20. J. F. Schumar *et al.*, *Fuel Element Failure Propagation Program Plan*, ANL/MET-01 (Aug 1969).
21. J. F. Perkins, *Energy Release from Decay of Fission Products*, Nucl. Sci. Eng. 3 (1958).